A structured approach for the engineering of biochemical network models, illustrated for signalling pathways*

Rainer Breitling[1], David Gilbert[2], Monika Heiner[3], Richard Orton[2]

[1] Groningen Bioinformatics Centre
University of Groningen
9751 NN Haren, The Netherlands

[2] Bioinformatics Research Centre
University of Glasgow
Glasgow G12 8QQ, Scotland, UK

[3] Department of Computer Science
Brandenburg University of Technology
03013 Cottbus, Germany

r.breitling@rug.nl, {drg,rorton}@brc.dcs.gla.ac.uk,
monika.heiner@informatik.tu-cottbus.de

April 11, 2008

Abstract

Quantitative models of biochemical networks (signal transduction cascades, metabolic pathways, gene regulatory circuits) are a central component of modern systems biology. Building and managing these complex models is a major challenge that can benefit from the application of formal methods adopted from theoretical computing science. Here we provide a general introduction to the field of formal modelling, which emphasizes the intuitive biochemical basis of the modelling process, but is also accessible for an audience with a background in computing science and/or model engineering.

We show how signal transduction cascades can be modelled in a modular fashion, using both a qualitative approach – Qualitative Petri nets, and quantitative approaches – Continuous Petri Nets and Ordinary Differential Equations. We review the major elementary building blocks of a cellular signalling model, discuss which critical design decisions have to be made during model building, and present a number of novel computational tools that can help to explore alternative modular models in an easy

*Accepted for publication in Briefings in Bioinformatics

and intuitive manner. These tools, which are based on Petri net theory, offer convenient ways of composing hierarchical ODE models, and permit a qualitative analysis of their behaviour.

We illustrate the central concepts using signal transduction as our main example. The ultimate aim is to introduce a general approach that provides the foundations for a structured formal engineering of large-scale models of biochemical networks.

Contents

1 Motivation

Quantitative modelling of biological systems ranging from metabolic networks to signalling pathways has experienced a renaissance in recent years. Biologists have come to realize that to fully understand (and successfully manipulate) complex interacting systems a quantitative description of their dynamic behaviour is all but essential. However, they have also noted that a successful model not only has to reproduce the system behaviour correctly, but also must reflect its physical structure in a meaningful way. The most popular way to achieve this is by modelling with ordinary differential equations (ODEs), which have a well-established biophysical basis and straightforward molecular interpretation (see [SSP06] for a detailed review). Petri nets are a well established formal descriptive technique from Computer Science for modelling dynamic systems which have recently been applied to biological networks (see Chaouiya [Cha07] for an excellent review).

This paper aims to lay the foundations for a more structured approach for the engineering of large-scale models of biochemical networks, illustrated for signalling pathways. Our approach exploits both Ordinary Differential Equations and the method of Petri nets. The integrated discussion of differential equation modeling, which is familiar to most biologists, and the corresponding

structured approach enabled by continuous Petri nets, opens new perspectives that should be of broad relevance for system modelers in many areas of cell and molecular biology. The illustration of the central concepts are based on familiar signal transduction pathways and classical enzyme kinetics, in order to ensure that the relevant concepts are immediately accessible to the widest possible audience.

Appendix A gives a short explanation of continuous Petri nets in mathematical terms, but for the following discussion only an intuitive understanding of the main concepts is needed. Basically, Petri nets are bipartite graphs (networks) with two types of nodes, one corresponding to molecules ("places"), the other corresponding to reactions ("transitions"). This structure is very similar to the familiar representation of biochemical networks, such as the maps of the Kyoto Encyclopedia of Genes and Genomes (KEGG). The arcs (edges) connecting the nodes encode information about reaction stoichiometry, and the places encode the molecular concentration. In the continuous version of Petri nets, each transition node contains detailed information about the kinetics of the associated chemical reaction ("firing rate function"). Consequently, each continuous Petri net corresponds in a unique and well-defined way to a system of ODEs describing the biological system dynamics. The advantages of this and other features of Petri nets will be discussed in more detail in the rest of the tutorial.

When building an ODE model with, e.g., a model building tool such as Gepasi [Men93], model complexity can rapidly increase to a level that is difficult to manipulate. Computational tools that allow the modular construction and visualization of ODE models would be very helpful, see e.g. [GH04]. In addition, one usually faces a number of non-trivial design choices during model building. Even for a relatively simple model there may be many ways to describe its dynamic behaviour. In the present paper we introduce the major elementary building blocks of a cellular signalling model, discuss some exemplary design decisions that have to be made during model building, and present a number of novel computational tools that can help to explore alternative modular models in an easy and intuitive manner. These tools, which are based on Petri net theory, offer convenient ways of composing hierarchical ODE models, using a graphical user interface, and we will discuss their application in some detail.

The basic building block of any biological dynamic system is the enzymatic reaction: the conversion of a substrate into a product catalysed by an enzyme. Such enzymatic reactions can be used to describe metabolic conversions, the activation of signalling molecules and even transport reactions between various subcellular compartments. The simple enzymatic reaction can be represented in various ways, and we will use this fundamental example to illustrate our paper. Modular tools, like the Petri net approach described below, will help to explore the consequences of alternative designs.

2 Modelling enzymatic reactions

The simplest chemical reaction in a biochemical system is spontaneous decay, whereby a substance A decays to produce a substance B:

$$A \rightarrow B \ . \tag{1}$$

In general, biochemical reactions are reversible (i.e. they have forward and reverse reaction rates which may be quite similar), and can be illustrated by

$$A \rightleftharpoons B \ . \tag{2}$$

Besides the spontaneous reaction, there is the enzymatic reaction, in which an enzyme catalyses the conversion of one or more biochemical entities (the *substrates*) into others (the *products*). We can illustrate a simple enzymatic reaction involving one substrate A, one product B, and an enzyme E by

$$A \xrightarrow{E} B \ . \tag{3}$$

Enzymes greatly accelerate reactions in one direction (often by factors of at least 10^6), and most reactions in biological systems do not occur at perceptible rates in the absence of enzymes.

To support the graphical construction of larger models by instantiation and composition of graph components, we also provide the continuous Petri net representations for all building blocks. In the Petri net notation, each reaction is modelled by a transition, where the pre-places are all its substrates and the post-places all its products. An enzyme establishes a side-condition at the given abstraction level; therefore its place is connected to the catalysed reaction by two opposite arcs. Compare Figure 1 for the Petri net representation of the three basic building blocks according Equations 1–3 as well as for the combination of Equations 2 and 3, the enzymatic reversible reaction.

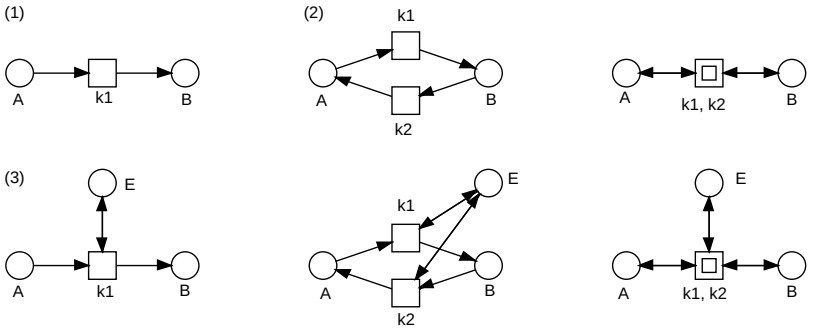

Figure 1: Building blocks corresponding to Equations 1–3 as Petri net components for irreversible (first column) and reversible (remaining columns) reactions, without (upper row) and with (lower row) explicitly modelled enzyme places. In the last column, the macro transitions, represented by two centric squares, stand for hierarchical nodes, hiding the two transitions of a reversible reaction on the next lower hierarchy level. In other words, the last column is just an abbreviation of the middle one. The labels k1 and k2 may be read as transition (reaction) identifiers, but they will also be interpreted as the kinetic parameters in the mass-action approach.

The Michaelis-Menten approach (MM)

In structural terms the reaction described by Equation 3 is particularly simple, because it does not require a detailed molecular understanding of the enzymatic reaction mechanism itself. Any kinetics that are just a function of the concentrations of A, B and E and some constant parameters will be compatible with this description. In practice, the *Michaelis-Menten* equation is commonly used when modelling enzymatic reactions. It is given in Equation MM

$$V = V_{\max} \times \frac{[A]}{K_M + [A]} \tag{MM}$$

where V is the reaction velocity, $V_{\max}$ is the maximum reaction velocity, and K_M, the *Michaelis constant*, is the concentration of the substrate at which the reaction rate is half its maximum value. The concentration of the substrate A is represented by $[A]$ in this rate equation. With the total enzyme concentration $[E_T]$ and the equation

$$k_{\text{cat}} = \frac{V_{\max}}{[E_T]} \tag{4}$$

we are able to write the differential equations describing the consumption of the substrate and production of the product as:

$$\frac{d[A]}{dt} = -\frac{d[B]}{dt} = -kcat \times [E_T] \times \frac{[A]}{(K_M + [A])} \tag{5}$$

That is exactly the result we get by assigning the Michaelis-Menten kinetics to the continuous transition labelled with k1 in subfigure (3) of Figure 1.

It is critical to note that the Michaelis-Menten equation only holds at the initial stage of a reaction before the concentration of the product is appreciable, and makes the following assumptions:

1. The concentration of product is (close to) zero.
2. No product reverts to the initial substrate.
3. The concentration of the enzyme is much less than the concentration of the substrate, i.e. $[E] \ll [A]$.

These are reasonable assumptions for enzyme assays in a test tube. However, assumptions 1 and 2 do not hold for most metabolic pathways *in vivo*, and none of the assumptions is correct for cellular signalling pathways. For instance, the concentration of kinases in a signalling cascade is about the same as the concentration of its downstream target, which usually is also a kinase. Also, reversibility and broad changes in substrate, enzyme and product concentration play an important role in cellular signalling pathways, requiring more detailed descriptions.

The mass-action approach (MA1)

A more detailed description can be given by taking into account the mechanism by which the enzyme acts, namely by forming a complex with the substrate, modifying the substrate to form the product, and a disassociation occurring to release the product, i.e. $A + E \rightleftharpoons AE \rightarrow B + E$. In order to take into account the kinetic properties of many enzymes, we associate *rate constants* with each reaction. Thus the enzyme E can combine with the substrate A to form the $A|E$ complex with rate constant k_1. The $A|E$ complex can dissociate to E and A with rate constant k_2, or form the product B with rate k_3:

$$A + E \underset{k_2}{\overset{k_1}{\rightleftarrows}} A|E \xrightarrow{k_3} B + E \ . \tag{MA1}$$

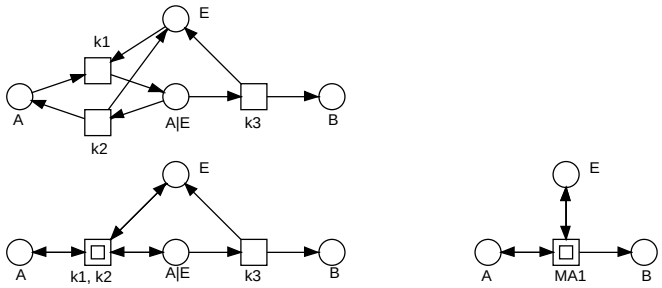

Figure 2: Building block **MA1** according Equation MA1 as Petri net component in three versions: flat (top left), 1-hierarchy (bottom left), 2-hierarchy (bottom right). Each of these building blocks, read as continuous Petri net, defines the system of differential equations as given in Equation 7.

This simple mass-action model is related to the Michaelis-Menten Equation MM as described previously by the following constraints:

$$\frac{k_2 + k_3}{k_1} = K_M \tag{6}$$

where $k_3 = k_{\text{cat}} = \frac{V_{\text{max}}}{[E_T]}$ as in Equation 4.

We can derive a set of differential equations from the mass-action description given in Equation MA1:

$$\begin{aligned}
\tfrac{d[A]}{dt} &= -k_1 \times [A] \times [E] \quad +k_2 \times [A|E] \\
\tfrac{d[A|E]}{dt} &= \ \ k_1 \times [A] \times [E] \quad -k_2 \times [A|E] \quad -k_3 \times [A|E] \\
\tfrac{d[B]}{dt} &= \qquad\qquad\qquad\qquad\qquad\quad +k_3 \times [A|E] \\
\tfrac{d[E]}{dt} &= -k_1 \times [A] \times [E] \quad +k_2 \times [A|E] \quad +k_3 \times [A|E]
\end{aligned} \tag{7}$$

These differential equations are derived in an obvious modular fashion from the underlying chemical equations, where each arrow connecting to a compound

corresponds to one term in the sum of the associated differential equation. Likewise, these differential equations are uniquely defined by the Petri net structure as given in Figure 2, if read as a continuous Petri net, compare Appendix. Obviously, the Petri net notation provides visualisation of the structure (topology), which is hidden in the ODEs.

The mass-action model described in Equation MA1 and Figure 2 assumes that almost none of the product reverts back to the original substrate, a condition that holds at the initial stage of a reaction before the concentration of the product is appreciable. This means that this type of mass-action model is a direct equivalent of the Michaelis-Menten equation, and will face the same limitations when applied to *in vivo* signalling systems. However, as we will show below, the mass-action description offers much more flexibility and thus can be easily expanded to cover more general situations.

More detailed mass-action descriptions of enzyme kinetics

The Michaelis-Menten equation and the corresponding mass-action model has been derived under the explicit assumption that there is no product present. It only holds for the initial rate of any enzymatic reaction. But almost all dynamical system models are concerned primarily with time-courses and/or steady-state behaviour. Both of these are clearly outside the range of the Michaelis-Menten approach and its corresponding mass-action model.

We can address this problem by formulating more detailed descriptions of enzymatic reactions using mass-action kinetics. Given that both substrate(s) and product(s) of an enzymatic reaction will bind to the same binding site, which often has the highest affinity for the transition state that is intermediate between substrate and product, it is reasonable to assume that the following extended version **MA2** of the reaction equations is a good approximation, see Figure 3 for the Petri net representation of this building block:

$$A + E \underset{k_2}{\overset{k_1}{\rightleftarrows}} A|E \xrightarrow{k_3'} B|E \underset{k_1'}{\overset{k_2'}{\rightleftarrows}} B + E \qquad \text{(MA2)}$$

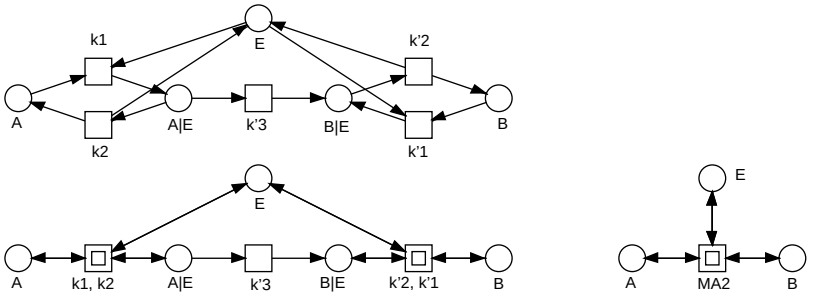

Figure 3: Building block **MA2** according Equation MA2 as Petri net component in three versions: flat (top left), 1-hierarchy (bottom left), 2-hierarchy (bottom right). Each of these building blocks, read as continuous Petri net, defines the same system of differential equations (not given).

The rate constants for the association and disassociation of the complex $B|E$ to $B + E$ are related to those for the association and disassociation of $A|E$, i.e. $k_1 \simeq k'_1$ and $k_2 \simeq k'_2$ because in general there will be only one bond change between the substrate A and the product B, while the overall conformation of the complexes $A|E$ and $B|E$ is maintained. Of course this assumption is a simplification, but it is made here without loss of generality. The only challenge then is to estimate k1 and k2, so that they fulfill the constraints in Equations 6 and 4 above, with the additional constraint that

$$k_3 = k_{\text{cat}} = \frac{k_2 * k'_3}{(k_2 + k'_3)} \tag{8}$$

assuming that the concentration of the enzyme-metabolite complexes is in steady state.

An even more complete mass-action model is given in Equation MA3, see Figure 4 for the corresponding Petri net representation of this building block. In this case the model describes in more detail the way in which the substrate is modified to form the product. The substrate first associates with the enzyme, and is then modified to form the product which is still associated with the enzyme. Finally the product and enzyme disassociate. All of the stages in the reaction are modelled as being reversible. An enzymatic reaction that is described by a certain set of Km/kcat values implies most strongly that its behaviour is governed in fact by equations MA2 and MA3 above. Any extension of Michaelis-Menten beyond time point 0 will be fraught with problems, as discussed earlier.

$$A + E \underset{k_2}{\overset{k_1}{\rightleftarrows}} A|E \underset{k'_4}{\overset{k'_3}{\rightleftarrows}} B|E \underset{k'_1}{\overset{k'_2}{\rightleftarrows}} B + E \tag{MA3}$$

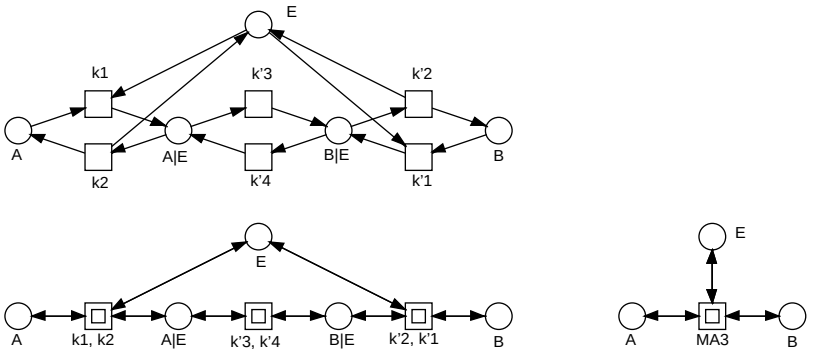

Figure 4: Building block **MA3** according Equation MA3 as Petri net component in three versions: flat (top left), 1-hierarchy (bottom left), 2-hierarchy (bottom right). Each of these building blocks, read as continuous Petri net, defines the system of differential equations (not given).

The differential equations for Equation MA2 and Equation MA3 can again be derived in an obvious modular fashion as demonstrated above for the mass-action pattern MA1, or – likewise – be generated out of the continuous interpre-

tation of the Petri net structures given in Figures 3 and 4 (compare Section 7 for a description of the tools used in our technology).

In Equation 9, based on Equation MA1, we give one description for the transformation of two substrates A_1 and A_2 into two corresponding products by the association first of A_1 with the enzyme and then the association of A_2 with the the complex formed by the first substrate and the enzyme. We model the disassociation and conversion into the two products in one step.

$$A_1 + A_2 + E \underset{k_{2_{A_1}}}{\overset{k_{1_{A_1}}}{\rightleftarrows}} A_1|E + A_2 \underset{k_{2_{A_2}}}{\overset{k_{1_{A_2}}}{\rightleftarrows}} A_1|A_2|E \xrightarrow{k_3} B_1 + B_2 + E \qquad (9)$$

Basic building blocks give us the ability to construct quite complex models, on a textual level by composing equations, or in a graphical way by composing Petri net components. Thus, for example the description of the RKIP influenced ERK signalling pathway is described by Cho et al. [CSK+03] employing an ODE description based on Equation 9 and two equations of the form given in Equation MA1. A corresponding Petri net representation is given in [GH04].

The decision of what granularity should be used to describe biochemical equations will largely be driven by the availability of kinetic data – the high granularity of mass-action descriptions will often require data on rate constants which cannot be obtained from the literature or experiments. A Michaelis-Menten description is often the most pragmatic choice even though it may yield misleading results in terms of simulation and analysis.

3 Signal transduction cascades

Once we have found the suitable description of the fundamental building blocks of a cellular system, i.e. the enzymatic reactions, we can combine them into more complex networks. In this paper we will focus on signal transduction cascades as an example, to illustrate the important principles of compositionality and modularity in cellular systems. It should be understood that each individual step in the cascade can be modelled by any of the basic types of building blocks introduced above. Hence, hybrid models are allowed and often reasonable, for example if the information about kinetic parameters is available at different levels of detail. In the following we give illustrative models in template form only, i.e. without reference to actual protein and specific rate constants; the interested reader is referred to [OSV+05] for descriptions of some models of the receptor tyrosine kinase activated MAPK signalling pathway.

Signal transduction is the mechanism that controls cellular responses to changes in the environment, including those changes that are generated by the organism itself, such as changes in hormone or growth factor concentrations. Extracellular signalling molecules bind to specific trans-membrane proteins (receptors), changing their conformation. This conformation change leads to a change in enzymatic activity of the receptor, which in turn affects the concentration of downstream compounds (the substrates and products of the reaction

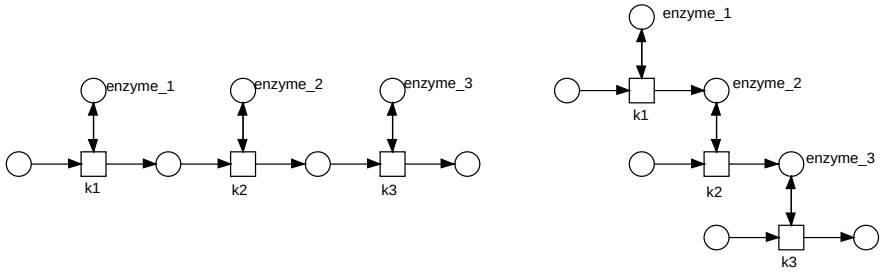

Figure 5: The essential structural difference between metabolic networks (left) and signal transduction networks (right) in terms of Petri net structures.

catalysed by the receptor). The downstream compounds may themselves be enzymes that in a cascade of enzymatic reactions ultimately lead to a change in gene expression or some other major adjustment of cellular physiology. These events, and the molecules that they involve, are referred to as (intracellular) "signalling pathways"; they are central to processes such as proliferation, cell growth, movement, apoptosis, and inter-cellular communication. The effect of "signalling cascades" which comprise a series of enzymatic reactions in which the product of one reaction acts as the catalytic enzyme for the next can be amplification of the original signal. However, in some cases, for example the MAP kinase cascade, the signal gain is modest [SEJGM02], suggesting that a main purpose, over and above relaying the signal, is regulation [KCG05] which may be achieved by positive and negative feedback loops (see below).

The main factor which distinguishes signal transduction pathways from metabolic networks is that in the former the product of an enzymatic reaction becomes the enzyme for the next step in the pathway, whereas in the latter the product of one reaction becomes the substrate for the next, see Figure 5. In general, it is *transient* behaviour which is of interest in a signalling pathway, as opposed to the steady state in a metabolic network. In gene regulatory networks, on the other hand, the inputs are proteins such as transcription factors (produced from signal transduction or metabolic activity), which then influence the expression of genes – enzymatic activity plays no direct role here. However, the products of gene regulatory networks can play a part in the transcription of other proteins, or can act as enzymes in signalling or metabolic pathways.

The first model of the ERK signalling cascade (the prototypical eukaryotic signal transduction pathway [BH05, WSL03]) was published in 1996 and utilised standard mass action kinetics (MA1) to represent the activation (phosphorylation) and deactivation (dephosphorylation) of the protein kinases [HF96]. Although relatively small (11 reactions and 18 species), the model was effectively used to investigate if the cascade exhibited ultrasensitivity. However, the next model of the ERK cascade utilised purely Michaelis-Menten type kinetics (MM) and was used to investigate whether the activation of ERK by MEK was processive or distributive [BS97]. Therefore, this shows that the different kinetic modelling approaches have both been employed from the very beginning of signal transduction modelling.

Over the past decade, an ever increasing number of models of the ERK

cascade have been developed, growing in both size and complexity through the years. Models now routinely incorporate growth factor receptors and the plethora of adaptor proteins that can bind to them and subsequently activate the core ERK cascade. However, like their predecessors, these models still utilise the standard mass action or Michaelis-Menten type kinetics (or a mixture of both) to represent the biochemical reactions of a system. One of the earliest models of the Epidermal Growth Factor Receptor (EGFR), which activates the downstream ERK cascade, utilised a mixture of both kinetic modelling approaches to represent ligand/receptor and receptor/adaptor binding and activation [KDGH99]; in general, MM kinetics were used to represent dephosphorylation reactions whilst MA1 kinetics were used to represent binding/dissociation and phosphorylation reactions in this model. Similarly, the model of the EGFR-ERK system developed by [BF03] also utilised both kinetic modelling approaches. However, this time MM kinetics were more extensively employed, representing both phosphorylation and dephosphorylation reactions, whilst MA1 kinetics were used primarily for binding/dissociation reactions. In addition, models composed entirely of mass action kinetics [LBS00, CSK+03, SEJGM02, IBG+04] or entirely [Koh00] and almost entirely [BHC+04] of Michaelis-Menten kinetics have also been constructed and successfully applied to signalling pathways. In some cases, the choice of kinetic modelling approach is explained [YTY03] and tends to favour the mass action approach due to some of the assumptions used to derive the Michaelis-Menten equation. However, in most cases the choice of kinetic modelling approach and its implications is not discussed, and alternatives are not systematically explored. Exploiting the modular approach advocated here, such an exploration of model space would be much easier to implement and could become a natural step of model analysis strategies.

4 Modelling one step in the cascade

One step in a classical signal transduction cascade comprises the *phosphorylation* of a protein by an enzyme S which is termed a kinase, see Figure 6. It is the phosphorylated form R_p which can act as an enzyme to catalyse the phosphorylation of a further component in the cascades, see Figure 9(a).

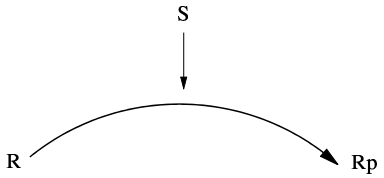

Figure 6: Basic enzymatic step; R – signalling protein; Rp – phosphorylated form; S1 – kinase

We can model this reaction using any of the kinetic patterns introduced in Section 2; e.g., the Mass Action **MA1** pattern as follows, straightforwardly adapted from Equation MA1 or equally its Petri net component given in Figure 2, by renaming in Equation 10, where R is a protein and R_p its phospho-

rylated form, S is a signal enzyme and $R|S$ the complex formed from R and S:

$$R + S \underset{k_2}{\overset{k_1}{\rightleftarrows}} R|S \xrightarrow{k_3} R_p + S \tag{10}$$

In order to ensure that such a single step is not a 'one shot' affair (i.e. to ensure that the substrate in the non-phosphorylated form is replenished and not exhausted), and hence that the signal can be deactivated where necessary, biological systems employ a phosphatase which is an enzyme promoting the de-phosphorylation of a phosphorylated protein. This is depicted in Figure 7, which we are going to model by all four introduced kinetic patterns.

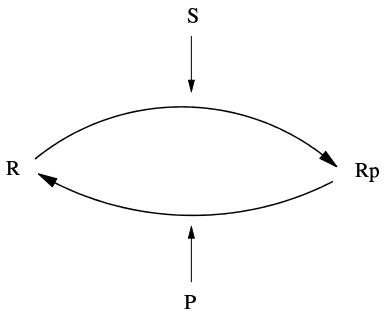

Figure 7: Basic phosphorylation–dephosphorylation step; R – signalling protein; Rp – phosphorylated form; S1 – kinase; P1 – phosphatase

We start with the mass-action patterns. Using the **MA1** pattern (Mass Action kinetics 1) we get Equation 11, where P is a phosphatase and k_n, kr_n are rate constants for the forward and reverse reactions respectively. In many cases it would also be justified to model the dephosphorylation as an un-catalysed first-order decay reaction, because detailed knowledge of phosphatase concentrations, specificities, and kinetic parameters is still lagging behind our understanding of the kinase enzymes.

$$\begin{aligned} R + S &\underset{k_2}{\overset{k_1}{\rightleftarrows}} R|S \xrightarrow{k_3} R_p + S \\ R + P &\xleftarrow{kr_3} R|P \underset{kr_2}{\overset{kr_1}{\rightleftarrows}} R_p + P \end{aligned} \tag{11}$$

We can construct a more complex description of the cascade step by utilising the more detailed formulation in Equation MA2 to give Equation 12 using **MA2** (Mass Action kinetics 2):

$$
\begin{aligned}
R + S \underset{k_2}{\overset{k_1}{\rightleftarrows}} R|S \xrightarrow{k'_3} R_p|S \underset{k'_1}{\overset{k'_2}{\rightleftarrows}} R_p + S \\
R + P \underset{kr_2}{\overset{kr_1}{\rightleftarrows}} R|P \xleftarrow{kr'_3} R_p|P \underset{kr'_1}{\overset{kr'_2}{\rightleftarrows}} R_p + P
\end{aligned}
\tag{12}
$$

A complete description in mass-action kinetics can be given by adapting Equation MA3 to give Equation 13 using **MA3** (Mass Action kinetics 3):

$$
\begin{aligned}
R + S \underset{k_2}{\overset{k_1}{\rightleftarrows}} R|S \underset{k'_4}{\overset{k'_3}{\rightleftarrows}} R_p|S \underset{k'_1}{\overset{k'_2}{\rightleftarrows}} R_p + S \\
R + P \underset{kr_2}{\overset{kr_1}{\rightleftarrows}} R|P \underset{kr'_4}{\overset{kr'_3}{\rightleftarrows}} R_p|P \underset{kr'_1}{\overset{kr'_2}{\rightleftarrows}} R_p + P
\end{aligned}
\tag{13}
$$

The Michaelis-Menten description **MM** for this reaction usually omits explicit reference to the phosphatase concentration because it is hard to measure; moreover because it is constant and not involved in any other reaction the term $-kcat \times [E_T]$ can be replaced by a single constant. Thus Equation 14 is modified for the reverse (dephosphorylation) reaction in Equation 14 to treat $[P]$ as a constant that is implicit in the kinetic constant k'_3:

$$
V = k_3 \times [S] \times \frac{[R]}{(K_{M1} + [R])} - k'_3 \times \frac{[R_p]}{(K_{M2} + [R_p])} \tag{14}
$$

where

- $\frac{d[R_p]}{dt}$ is the reaction rate V,
- $k_3 \times [S]$ is V_{max} for the forward reaction,
- k'_3 is V_{max} for the reverse reaction, and
- $K_{M1} = \frac{(k_2+k_3)}{k_1}$ with values from Equation 11.

Figure 8 summarizes the corresponding Petri net models for these four versions of the basic phosphorylation-dephosphorylation step.

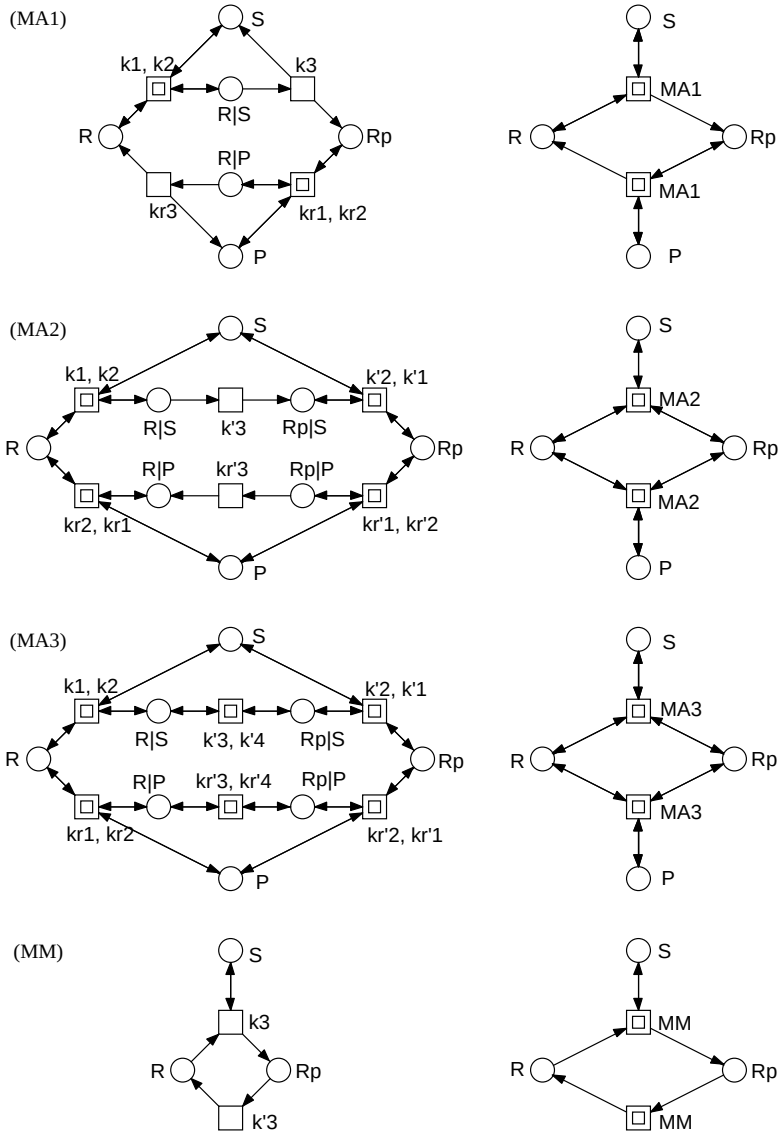

Figure 8: The Petri net representations (top hierarchy levels only) for Equations 11–14, re-using the components introduced in Figures 1–4. Each system is given in two versions. The right column provides the 2-hierarchy versions of the left column; i.e., both columns generate the same ODEs.

5 Composing kinase cascades using building blocks

Once we have defined the building blocks, we can compose them by chaining together basic phosphorylation–dephosphorylation steps.

Vertical and horizontal composition

Composition can be performed vertically as in Figure 9(a) to form a *signalling cascade*, where the signalling protein in the second stage is labelled RR and its phosphorylated form is labelled RR_p. Horizontal composition is illustrated in Figure 9(b) where a double phosphorylation step is described; the double phosphorylated form of a protein is subscripted by pp.

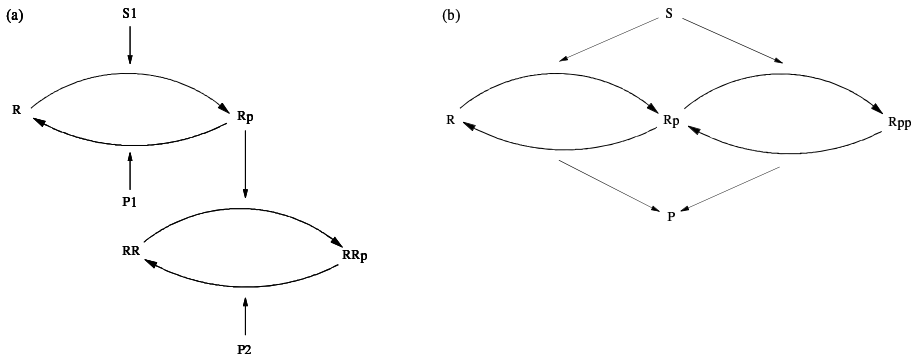

Figure 9: (a) Vertical composition: Cascade formed by chaining two basic phosphorylation-dephosphorylation steps. (b) Horizontal composition: One stage cascade with a single to double phosphorylation step.

We can again use any of the kinetic patterns that were previously introduced in order to derive the models. For example, using **MA1** we can represent a two-stage cascade illustrated in Figure 9(a) by the following mass-action equations, ignoring for the sake of simplicity the dephosphorylation steps in the textual representation. The rate constants associated with the second stage are labelled kk_n. We would not expect the dephosphorylation rate constants to be related to the phosphorylation rate constants.

$$\begin{aligned} R + S_1 &\underset{k_2}{\overset{k_1}{\rightleftarrows}} R|S_1 \xrightarrow{k_3} R_p + S1 \\ RR + R_p &\underset{kk_2}{\overset{kk_1}{\rightleftarrows}} RR|R_p \xrightarrow{kk_3} RR_p + R_p \end{aligned} \tag{15}$$

The complete two-stage cascade using the mass-action equation pattern MA1 gives rise to the ODEs given in Equation 16.

$$
\begin{aligned}
\tfrac{d[R]}{dt} &= -k_1 \times [R] \times [S_1] + k_2 \times [R|S_1] \\
\tfrac{d[R|S_1]}{dt} &= k_1 \times [R] \times [S_1] - k_2 \times [R|S_1] - k_3 \times [R|S_1] \\
\tfrac{d[R_p]}{dt} &= k_3 \times [R|S_1] \\
\tfrac{d[S_1]}{dt} &= -k_1 \times [R] \times [S_1] + k_2 \times [R|S_1] + k_3 \times [R|S_1] \\
\tfrac{d[RR]}{dt} &= -kk_1 \times [RR] \times [R_p] + kk_2 \times [RR|R_p] \\
\tfrac{d[RR|R_p]}{dt} &= kk_1 \times [RR] \times [R_p] - kk_2 \times [RR|R_p] - kk_3 \times [RR|R_p] \\
\tfrac{d[RR_p]}{dt} &= kk_3 \times [RR|R_p] \\
\tfrac{d[R_p]}{dt} &= -kk_1 \times [RR] \times [R_p] + kk_2 \times [RR|R_p] + kk_3 \times [RR|R_p]
\end{aligned}
\tag{16}
$$

The Michaelis-Menten description for this two-stage cascade is more compact than the ODE version above, and is given by Equation 17:

$$
\begin{aligned}
\tfrac{d[R_p]}{dt} &= k_3 \times [S_1] \times \tfrac{[R]}{(K_{M1}+[R])} - k_3' \times \tfrac{[R_p]}{(K_{M2}+[R_p])} \\
\tfrac{d[RR_p]}{dt} &= kk_3 \times [R_p] \times \tfrac{[RR]}{(K_{MM1}+[RR])} - kk_3' \times \tfrac{[RR_p]}{(K_{MM2}+[RR_p])}
\end{aligned}
\tag{17}
$$

The ODEs given in Equations 16 and 17 are defined by the continuous Petri nets given in Figure 10(b), using appropriately chosen kinetic patterns for the macro transitions.

The addition of a double phosphorylation step to a cascade layer is given in Figure 9(b), where both the single and double phosphorylation steps are catalysed by the same enzyme S; likewise, the two dephosphorylation steps are usually catalysed by the same phosphatase P. This system component can be described by Equation 18, if we apply the mass-action kinetics **MA1** and ignore again for the sake of simplicity the dephosphorylation steps in the textual representation. The rate constants associated with the double phosphorylation are labelled kp_n. Often, we can assume that the rate constants for the two steps of the double phosphorylation are similar to those for the single phosphorylation.

$$
\begin{aligned}
R + S &\underset{k_2}{\overset{k_1}{\rightleftarrows}} R|S \xrightarrow{k_3} R_p + S \\
R_p + S &\underset{kp_2}{\overset{kp_1}{\rightleftarrows}} R_p|S \xrightarrow{kp_3} R_{pp} + S
\end{aligned}
\tag{18}
$$

The ODEs for the double phosphorylation can be generated by the continuous Petri net given in Figure 10(c), where the kinetic patterns for the macro transitions have to be adjusted appropriately.

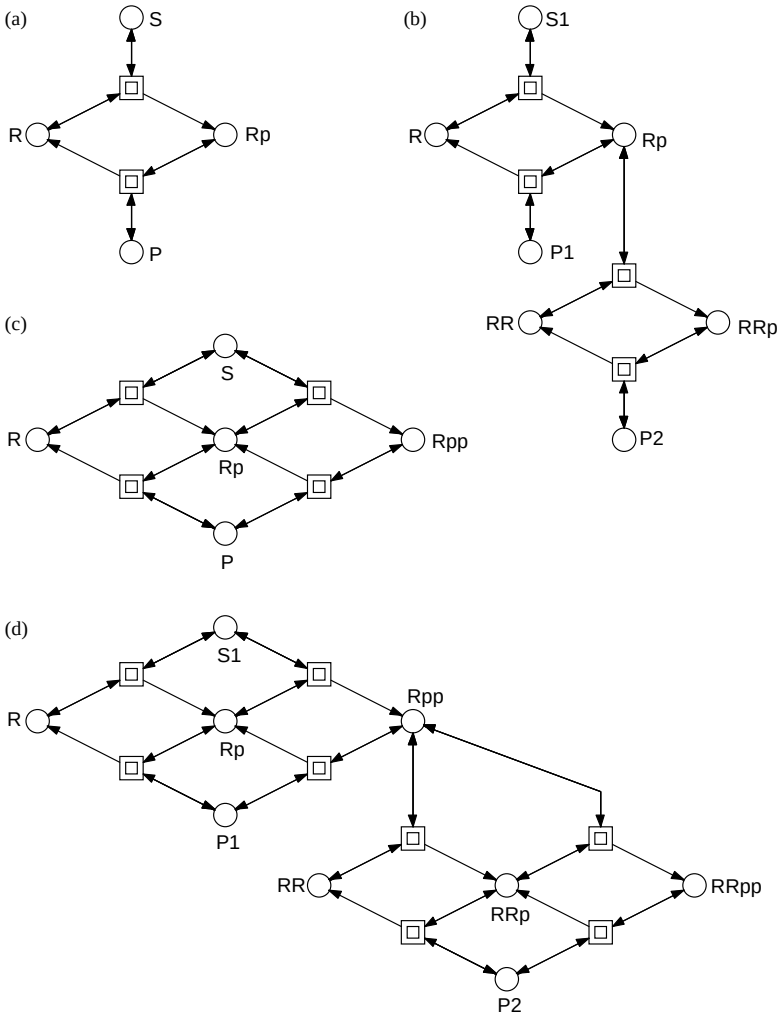

Figure 10: Starting from the building block (a) for the basic phosphorylation-dephosphorylation step (as defined in four versions in Figure 8), we can do vertical composition forming signalling cascades, as given in (b), and horizontal composition, resulting in the structure (c) for the double phosphorylation. Applying both composition principles yields the two-stage double phosphorylation cascade as given in (d).

Negative and positive feedback

Feedback in a signalling network can be achieved in several ways. For example, negative feedback can be implemented at the molecular level by sequestration of the input signal S_1 by the product of the second stage RR_p. This system is sketched in Figure 11(a), and can be achieved by combining equations 15 and 19. See Figure 12(a) for the continuous Petri net, from which the ODEs can be derived; of course, these need to be completed by the dephosphorylation equations (this is equally true for all the structures discussed in the following).

Similarly, positive feedback can also be achieved by the sequestration of the input signal S_1 by the product of the second stage, under the additional condition that the resulting $S_1|RR_p$ complex is a more active enzyme than S_1 alone. In this case we add Equation 20 to equations 15 and 19. The system is sketched in Figure 11(b), and the continuous Petri net is given in Figure 12(b), from which the ODEs can be derived.

$$S_1 + RR_p \underset{i_2}{\overset{i_1}{\rightleftarrows}} S_1|RR_p \tag{19}$$

$$R + S_1|RR_p \underset{kp_2}{\overset{kp_1}{\rightleftarrows}} R|S_1|RR_p \xrightarrow{kp_3} R_p + S_1|RR_p \tag{20}$$

Many other molecular mechanisms can be envisaged and are in fact observed in biological systems. All of these can be represented using the same basic formalism. For example, we can model an influence of RR_p on the phosphatase P_1, in which case the effects of positive and negative feedback are reversed, i.e. sequestration of P_1 by RR_p can cause positive feedback – see Figure 11(c). This can be achieved with Equations 15 and 21. Alternatively the situation where the $P_1|RR_p$ complex is more active than P_1 will cause negative feedback, Figure 11(d), and can be described by adding Equation 22 to Equations 15 and 21.

$$P_1 + RR_p \underset{i_2}{\overset{i_1}{\rightleftarrows}} P_1|RR_p \tag{21}$$

$$R_p + P_1|RR_p \underset{kr'_2}{\overset{kr'_1}{\rightleftarrows}} R_p|P_1|RR_p \xrightarrow{kr'_3} R + P_1|RR_p \tag{22}$$

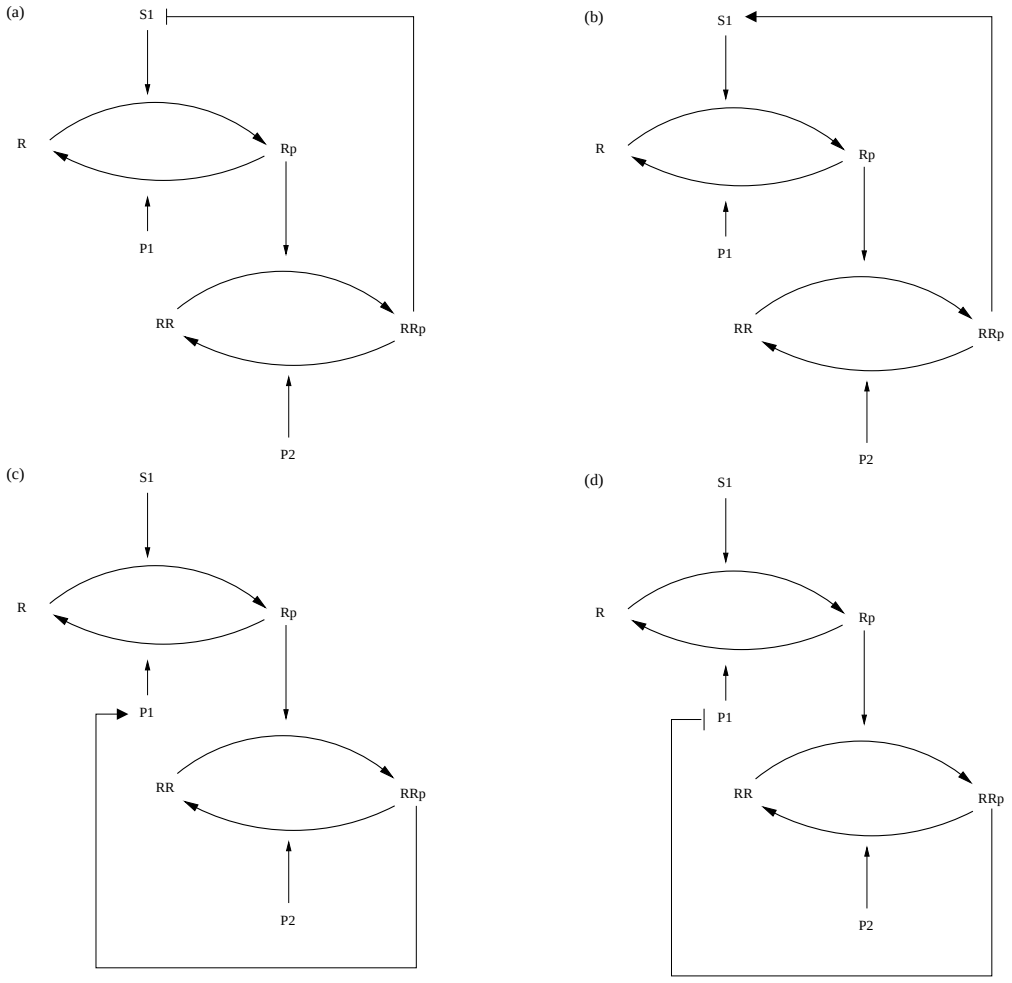

Figure 11: Two-stage cascade with (a) negative feedback, (b) positive feedback; alternative two-stage cascade with (c) negative feedback, (d) positive feedback.

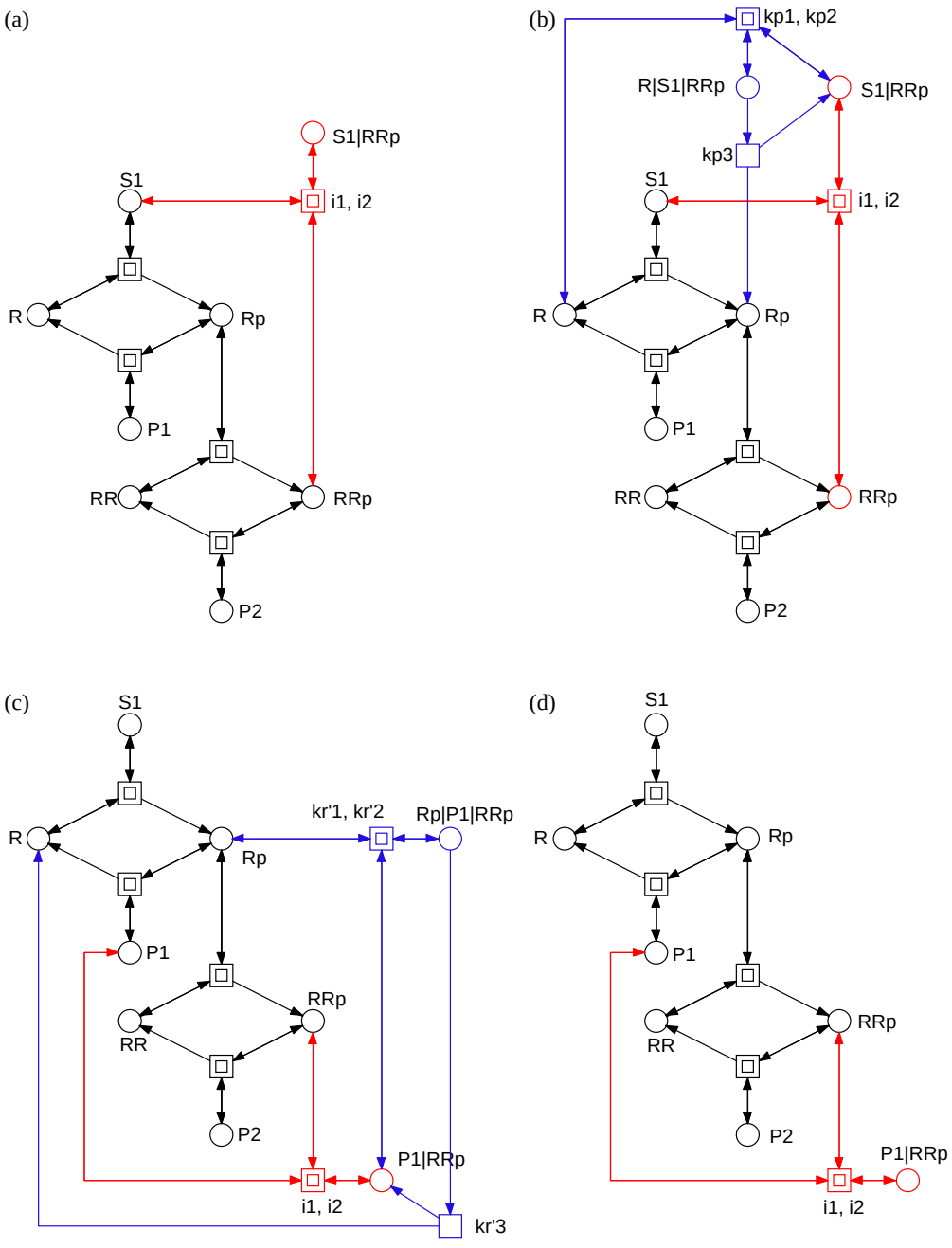

Figure 12: Petri nets, corresponding to Figure 11, for a two-stage cascade with (a) negative feedback, (b) positive feedback (the reaction sequence i_1, kp_1, kp_3 contributes to the phosphorylation); alternative two-stage cascade with (c) negative feedback (the reaction sequence i_1, kr'_1, kr'_3 contributes to the dephosphorylation), (d) positive feedback.

6 Analysing the behaviour of the models

Clearly the construction of models of a biochemical system has to be done with some purpose in mind. Overall, the main motivation will often be to provide some guidance to biochemists regarding the way in which they could carry out the exploration, modification or (re-)construction of a biological system of interest. Such advice could contribute towards the optimisation of resources (human, fiscal) and time in terms of the choice and temporal ordering of what assays to perform. The usefulness of the models will depend on their ability to provide an unambiguous representation of the knowledge about the biochemical system, obtained from interviewing the biologists, searching the literature as well as experimental data from biochemical experiments. Thus a major task in model construction is interaction with biologists in order to ensure that the correct model is built.

Models should be able to provide biochemists with a foil against which to test their understanding of a biological system – initially the components and how they interact (network topology), and then regarding aspects of the behaviour of the system. In the first instance, the explanatory power of a model is related to its ability to represent and explain everything that is known about the biological system, under various conditions. Furthermore, the usefulness of the explanatory power of a model is often linked to its capability to correctly predict the behaviour of a system under new (as yet unseen) conditions which will be achieved by new biological assays.

The first check that should be carried out on a model of a biochemical network is whether it correctly describes the *components and their relationships* at an adequate level of detail. This should be done with biochemists who will often represent the system of interest in some diagram with more or less formality and internal consistency. The initial task for the modeller is thus to create an abstract, qualitative representation of a biochemical network, minimally described by its topology, usually as a bipartite directed graph with nodes representing biochemical entities or reactions, or in Petri net terminology *places* and *transitions*. Arcs can be annotated with stoichiometric information.

The *qualitative description* can be further enhanced by the abstract representation of discrete quantities of species, achieved in Petri nets by the use of tokens at places. These can represent the number of molecules, or the discrete level of concentration, of a species. A particular arrangement of tokens over a network is called a *marking*. The firing rule brings the tokens to life. Their motion through the network (token animation) can be visualized by playing the token game, which allows to experience model behaviour. The standard semantics for these qualitative Petri nets (QPN) does not associate a time with transitions or the sojourn of tokens at places, and thus these descriptions are time-free. The qualitative analysis considers, however, all possible types of behaviour of the system under any timing. The behaviour of such a net forms a discrete state space, which can be analysed in the bounded case, for example, by a branching time temporal logic, one instance of which is Computational Tree Logic (CTL); see [CGP01] and the Model Checking Kit [SSE03] for collections of suitable model checkers. Qualitative analyses may also be made using

classical Petri net theory, as provided, e.g., by the Integrated Net Analyser INA [SR99]. The partial order behaviour as provided by qualitative Petri nets can contribute to deeper insights into the signal-response behaviour of signalling networks, as demonstrated in [GHL07].

Timed information can be added to the qualitative description in two ways – stochastic and continuous. [GH04], [GHL07] provide case studies, demonstrating the complementary application of qualitative as well as *quantitative models* to a common biological system. It should be borne in mind that time assumptions generally impose constraints on behaviour. Thus qualitative models consider all possible behaviours under any timing, whereas continuous models are constrained by their inherent determinism to consider a subset. This may be too restrictive when modelling biochemical systems, which by their very nature exhibit variability in their behaviour and a stochastic approach may be more suitable. However, in this paper for reasons of space we ignore the stochastic view, and refer the reader to [GHL07] for a description of stochastic Petri nets and their relationship to qualitative and continuous models.

The *continuous model* replaces the discrete values of species with continuous values, and hence is not able to describe the behaviour of species at the level of individual molecules, but only the overall behaviour via concentrations. We can regard the discrete description of concentration levels as abstracting over the continuous description of concentrations. Timed information is introduced by the association of a particular deterministic rate information with each transition, permitting the continuous (Petri net) model to be represented as a set of ordinary differential equations (ODEs). The concentration of a particular species in such a deterministic model will have the same value at each point of time for repeated computational simulations.

(Qualitative) Petri nets and ODEs do share some concepts, as e.g. the notions of P-invariants and T-invariants, see [Mur89], which are known in the continuous world under the terms mass conservation or stationary flux, elementary mode, extreme pathway, respectively, see [Pal06]. Because qualitative and quantitative models share the structure, it is likely that they share some behaviour, too. Thus, [ADLS07] presents a qualitative Petri net approach to persistence analysis in (continuous) chemical reaction networks.

Systems of ODEs are often non-linear, and not amenable to analytical solution methods, thus numerical methods must be used. In addition, the ODEs can describe a *stiff* system and stiff ODE solvers need to be used. Such solutions give traces of the deterministic behaviour of the concentrations of biochemical species over time, from which for example input–output (signal–response) behaviour can be computed. One common task is to fit the behaviour of a model to the observed data, essentially undertaking system identification which can be done both in terms of the qualitative as well as quantitative aspects. The latter can be achieved in a semi-manual manner by parameter scanning or by more automatic methods based on optimisation. However, laboratory data is often sparse in terms of time points, does not contain the results of many repeated experiments, and is highly variable. This presents a particular challenge to modelling, and it is an ongoing area of research to develop appropriate data-fitting techniques. The automated performance of qualitative model identification (i.e.

the choice of suitable topologies to describe a system), in conjunction with the derivation of kinetic data is a difficult task.

The state space of such models is continuous and linear and can be analysed, for example, by Linear Temporal Logic with constraints (LTLc) as provided by the Biocham tool [CCRFS06]. Besides the numerical evaluation of ODEs, the qualitative analysis of their solutions are often of interest, as analysis of (the existence of) equilibria and stability, oscillation, persistency, sensitivity and bifurcation [Gle94]. ODEs are also commonly used in the classical metabolic control analysis [HS96], which aims at a quantification in terms of control coefficients to determine the extent to which different enzymes limit the flux under particular conditions.

7 Tools

Several tools are available which permit the construction of qualitative biochemical pathway models using kinetic descriptions and their simulation and analysis; these often read and write in SBML [HFS+03] format which is one de-facto standard for the description of quantitative models of biochemical pathways. Such tools include BioNessie [Bio], and Copasi [HSG+06]. MATLAB [SR97] is a high-level language and interactive environment which contains a large number of ODE solvers which can be used to numerically solve and analyse ODEs. The SimBiology toolbox extends MATLAB with tools for modelling, simulating, and analyzing biochemical pathways, and has an interface which can read and write SBML. The Systems Biology Workbench (SBW) [BS06], is a software framework that includes Jarnac, a fast simulator of reaction networks, permitting time course simulation (ODE or stochastic), steady state analysis, basic structural properties of networks, dynamic properties like the Jacobian, elasticities, sensitivities, and eigenvalues, and JDesigner, a friendly GUI front end to an SBW compatible simulator. Bifurcation analysis can be performed conveniently using Xppaut [Erm02].

In this paper, the (continuous) Petri net models have been designed using Snoopy [Sno], a tool to design and animate hierarchical graphs, especially Petri nets. Snoopy supports qualitative as well as quantitative Petri nets, among them continuous Petri nets. Snoopy's export feature opens the door to various analysis tools, comprising tools devoted to standard Petri net theory, e.g. INA [SR99], as well as a variety of model checkers, e.g. the Model Checking Kit [SSE03]. There is also an export to SBML [HFS+03], allowing access to other tools for more detailed evaluations of continuous Petri nets in addition to the standard algorithms of ODE solvers provided by Snoopy. Moreover, the ODEs defined by a continuous Petri net can be generated in LATEX style, see Appendix B for examples.

All the continuous Petri nets introduced in this paper, and by this way all the ODEs defined by them, are available at

www-dssz.informatik.tu-cottbus.de/examples/ode_tutorial .

8 Summary

In this paper we have shown how signal transduction cascades can be modelled in a modular fashion, using Qualitative and Continuous Petri Nets, and Ordinary Differential Equations. We have reviewed the major elementary building blocks of a cellular signalling model, described some basic network topologies, and discussed which critical design decisions have to be made during model building. We have also presented a number of novel computational tools that can help to explore alternative modular models in an easy and intuitive manner. These tools, which are based on Petri net theory, offer convenient ways of composing hierarchical ODE models, and permit a qualitative analysis of their behaviour.

With these tools and the concepts introduced in this paper, readers should be able to start their journey into the exciting area of formal computational systems biology. We hope to have shown that there are many interesting challenges yet to be solved, and that a structured principled approach will be essential for tackling them.

Our longer-term goal is that the concepts described in this paper will contribute to a general approach that provides the foundations for a structured formal engineering of large-scale models of biochemical networks.

Acknowledgements

This work has been partially supported by the Beacons Post Genomics grant QCBB/C.012/00010 from the Department of Trade and Industry (UK) and European Union FP6 STREP project 027265.

References

[ADLS07] D. Angeli, P. De Leenheer, and E.D. Sontag. A petri net approach to persistence analysis in chemical reaction networks. In G. Garcia I. Queinnec, S. Tarbouriech and (eds.) S.-I. Niculescu, editors, *Biology and Control Theory: Current Challenges, Lecture Notes in Control and Information Sciences*, pages 181–216. Springer, 2007.

[BF03] F.A. Brightman and D.A. Fell. Differential feedback regulation of the MAPK cascade underlies the quantitative differences in EGF and NGF signalling in PC12 cells. *FEBS Lett*, 482(3):169–174, 2003.

[BH05] R. Breitling and D. Hoeller. Current challenges in quantitative modeling of epidermal growth factor signaling. *FEBS Lett*, 579(28):6289–94, 2005.

[BHC+04] K.S. Brown, C.C. Hill, G.A. Calero, C.R. Myers, K.H. Lee, J.P. Sethna, and R.A. Cerione. The statistical mechanics of complex signaling networks: nerve growth factor signaling. *Phys Biol*, 1(3–4):184–195, 2004.

[Bio] BioNessie. A biochemical pathway simulation and analysis tool. University of Glasgow, www.bionessie.org.

[BS97] W.R. Burack and T.W. Sturgill. The activating dual phosphorylation of MAPK by MEK is nonprocessive. *Biochemistry*, 36(20):5929–33, 1997.

[BS06] F. T. Bergmann and H. M. Sauro. SBW - a modular framework for systems biology. In L. F. Perrone, B. Lawson, J. Liu, and F. P. Wieland, editors, *Winter Simulation Conference*, pages 1637–1645. WSC, 2006.

[CCRFS06] L. Calzone, N. Chabrier-Rivier, F. Fages, and S. Soliman. Machine learning biochemical networks from temporal logic properties. In *T. Comp. Sys. Biology VI, LNCS 4220*. Springer, 2006.

[CGP01] E.M. Clarke, O. Grumberg, and D.A. Peled. *Model checking*. MIT Press 1999, third printing, 2001.

[Cha07] Claudine Chaouiya. Petri net modelling of biological networks. *Briefings in Bioinformatics*, 8(4):210–219, 2007.

[CSK+03] K.-H. Cho, S.-Y. Shin, H.-W. Kim, O. Wolkenhauer, B. McFerran, and W. Kolch. Mathematical modeling of the influence of RKIP on the ERK signaling pathway. *Lecture Notes in Computer Science*, 2602:127–141, 2003.

[DA05] R. David and H. Alla. *Discrete, Continuous, and Hybrid Petri Nets*. Springer, 2005.

[Erm02] B. Ermentrout. *Simulating, Analyzing, and Animating Dynamical Systems: A Guide to Xppaut for Researchers and Students (Software, Environments, Tools)*. SIAM, 2002.

[GH04] D. Gilbert and M. Heiner. From Petri Nets to Differential Equations - an Integrative Approach for Biochemical Network Analysis;. In *Proc. 27th ICATPN 2006, LNCS 4024*, pages 181–200. Springer, 2004.

[GHL07] D. Gilbert, M. Heiner, and S. Lehrack. A unifying framework for modelling and analysing biochemical pathways using Petri nets. In *Proc. CMSB 2007, LNCS/LNBI 4695*, pages 200–216. Springer, 2007.

[Gle94] P. Glendinning. *Stability, Instability, and Chaos: an Introduction to the Theory of Nonlinear Differential Equations*. Cambridge University Press, 1994.

[HF96] C.Y. Huang and J.E. Ferrell. Ultrasensitivity in the mitogen-activated protein kinase cascade. *Proc Natl Acad Sci U S A*, 93(19):10078–83, 1996.

[HFS+03] M. Hucka, A. Finney, H. M. Sauro, H. Bolouri, J. C. Doyle, H. Kitano, and et al. The systems biology markup language (SBML): A medium for representation and exchange of biochemical network models. *Bioinformatics*, 19:524–531, 2003.

[HS96] R. Heinrich and S. Schuster. *The Regulation Of Cellular Systems*. Springer, 1996.

[HSG+06] S. Hoops, S. Sahle, R. Gauges, C. Lee, J. Pahle, N. Simus, M. Singhal, L. Xu, P. Mendes, and U. Kummer. COPASI - a COmplex PAthway SImulator. *Bioinformatics*, 22(24):3067–3074, 2006.

[IBG+04] A.E. Ihekwaba, D.S. Broomhead, R.L. Grimley, N. Benson, and DB. Kell. Sensitivity analysis of parameters controlling oscillatory signalling in the NF-kappaB pathway: the roles of IKK and IkappaBalpha. *Syst Biol (Stevenage)*, 1(1):93–103, 2004.

[KCG05] W. Kolch, M. Calder, and D. Gilbert. When kinases meet mathematics: the systems biology of MAPK signalling. *FEBS Lett.*, 579(8):1891–5, 2005.

[KDGH99] B.N. Kholodenko, O.V. Demin, Moehren G., and J.B. Hoek. Quantification of short term signaling by the epidermal growth factor receptor. *J Biol Chem*, 274(42):30169–81, 1999.

[Koh00] B.N. Koholodenko. Negative feedback and ultrasensitivity can bring about oscillations in the mitogen-activated protein kinase cascades. *Eur J Biochem*, 267(6):1583–1588, 2000.

[LBS00] A. Levchenko, J. Bruck, and P.W. Sternberg. Scaffold proteins may biphasically affect the levels of mitogen-activated protein kinase signaling and reduce its threshold properties. *Proc Natl Acad Sci U S A*, 97(11):5818–23, 2000.

[Men93] P. Mendes. GEPASI: A software package for modelling the dynamics, steady states and control of biochemical and other systems. *Comput Applic Biosci*, 9:563–571, 1993.

[Mur89] T. Murata. Petri Nets: Properties, Analysis ans Applications. *Proc.of the IEEE 77*, 4:541–580, 1989.

[OSV+05] R. Orton, O. Sturm, V. Vyshemirsky, M. Calder, D. Gilbert, and W. Kolch. Computational Modelling of the Tyrosine Receptor Kinase Activated MAPK Pathway. *Biochem J*, 392:249–261, 2005.

[Pal06] B. Ø. Palsson. *Systems Biology, Properties of Reconstructed Networks*. Cambridge University Press, 2006.

[SEJGM02] B. Schoeberl, C. Eichler-Jonsson, E.D. Gilles, and G. Muller. Computational modeling of the dynamics of the MAP kinase cascade activated by surface and internalized EGF receptors. *Nature Biotech*, 20:370–375, 2002.

[Sno] Snoopy. A tool to design and animate hierarchical graphs. BTU Cottbus, CS Dep., www-dssz.informatik.tu-cottbus.de.

[SR97] L. F. Shampine and M. W. Reichelt. The MATLAB ODE Suite. *SIAM Journal on Scientific Computing*, 18:1–22, 1997.

[SR99] P.H. Starke and S. Roch. Ina - The Intergrated Net Analyzer. Technical report, Humboldt University Berlin, http://www.informatik.hu-berlin.de/∼starke/ina.html, 1999.

[SSE03] C. Schröter, S. Schwoon, and J. Esparza. The Model Checking Kit. In *Proc. ICATPN, LNCS 2679*, pages 463–472. Springer, 2003.

[SSP06] Z. Szallasi, J. Stelling, and V. Periwal. *System Modeling In Cellular Biology. From Concepts to Nuts and Bolts*. MIT Press, 2006.

[WSL03] H. S Wiley, S. Y. Shvartsman, and D. A. Lauffenburger. Computational modeling of the EGF-receptor system: a paradigm for systems biology. *Trends Cell Biol*, 13(1):43–50, 2003.

[YTY03] S. Yamada, T. Taketomi, and A. Yoshimura. Model analysis of difference between EGF pathway and FGF pathway. *Biochem Biophys Res Commun*, 314(4):1113–1120, 2003.

Appendix A: Continuous Petri Nets

Continuous Petri nets are a quantified version of the standard notion of qualitative Petri nets, see e.g. [Mur89]. Like their ancestor, they are weighted, directed, bipartite graphs with the following basic ingredients.

- There are two types of nodes, which are called (continuous) places $P = \{p_1, \ldots, p_m\}$, in the figures represented by circles, and (continuous) transitions $T = \{t_1, \ldots, t_n\}$, in the figures represented by rectangles. Places usually model passive system components like species, while transitions stand for active system components like reactions.
- The directed arcs connect always nodes of different type.
- Arcs are weighted by non-negative real numbers, whereby the arc weight may be read as the multiplicity of the arc. The arc weight 1 is the default value and is usually not given explicitly.
- Each place gets a non-negative real number, called token value, which we interpret as the concentration of a given species. The token values of all places establish the marking of the net, which represents the current state of the system.

To be precise we give the following definition.

Definition 8.1 (Continuous Petri net) *A* continuous Petri net *is a quintuple* $\mathcal{CON} = \langle P, T, f, v, m_0 \rangle$*, where*

- P *and* T *are finite, non empty, and disjoint sets.* P *is the set of* continuous places*.* T *is the set of* continuous transitions*.*
- $f : ((P \times T) \cup (T \times P)) \to \mathbf{R}_0^+$ *defines the set of directed* arcs*, weighted by non-negative real numbers.*
- $v : T \to H$ *assigns to each transition a* firing rate function*, whereby* $H := \bigcup_{t \in T} \left\{ h_t | h_t : \mathbf{R}^{|{}^\bullet t|} \to \mathbf{R} \right\}$ *is the set of all firing rate functions, and* $v(t) = h_t$ *for all transitions* $t \in T$*.*
- $m_0 : P \to \mathbf{R}_0^+$ *gives the* initial marking*.*

The function $v(t)$ defines the marking-dependent transition rate for the transition t. The domain of $v(t)$ is restricted to the set of pre-places of t, i.e. ${}^\bullet t := \{p \in P | f(p,t) \neq 0\}$, to enforce a close relation between network structure and transition rate functions. Therefore $v(t)$ actually depends only on a sub-marking. Technically, any mathematical function in compliance with this restriction is allowed for $v(t)$. However, often special kinetic patterns are applied, whereby Michaelis-Menten and mass-action kinetics seem to be the most popular ones.

The behaviour of a continuous Petri net is defined by the following. A continuous transition t is enabled at m, iff $\forall p \in {}^\bullet t : m(p) > 0$. Due to the influence

of time, a continuous transition is forced to fire as soon as possible. The instantaneous firing of a transition is carried out like a continuous flow, whereby the strength of the flow is determined by the firing rate function.

Altogether, the semantics of a continuous Petri net is defined by a system of ordinary differential equations (ODEs), where one equation describes the continuous change over time on the token value of a given place by the continuous increase of its pre-transitions' flow and the continuous decrease of its post-transitions' flow, i.e., each place p subject to changes gets its own equation:

$$\frac{m\left(p\right)}{dt} = \sum_{t \in {}^\bullet p} f\left(t,p\right) v\left(t\right) - \sum_{t \in p^\bullet} f\left(p,t\right) v\left(t\right).$$

The notation ${}^\bullet p$ specifies the set of pre-transitions of p, i.e. all reactions producing the species p: ${}^\bullet p := \{t \in T | f\left(t,p\right) \neq 0\}$,
and $p^\bullet$ specifies the set of post-transitions of p, i.e. all reactions consuming the species p: $p^\bullet := \{t \in T | f\left(p,t\right) \neq 0\}$.

The notation $m(p)$ refers to the current token value of place p, and corresponds to the more popular notation $[p]$. To simplify the notation in the generated ODEs, places are usually interpreted as (non-negative) real variables, which allows to write, e.g., $v(A,B)$ instead of $v(m(A),m(B))$ or $v([A],[B])$.

Each equation corresponds basically to a line in the incidence matrix (stoichiometric matrix), whereby now the matrix elements consist of the rate functions multiplied by the arc weight, if any. Moreover, as soon as there are transitions with more than one pre-place, we get typically a non-linear system, which calls for a numerical treatment of the system on hand.

With other words, the continuous Petri net becomes the structured description of the corresponding ODEs. Due to the explicit structure we expect to get descriptions which are less error prone compared to those ones created manually in a textual notation from the scratch. For more details see [GH04], and for a family of related models see [DA05].

Appendix B: Complete Example Nets

In the following we give six models of a three-stage signalling cascade, demonstrating the composition principle using building blocks. First, the basic models for in vivo and in vitro cascades are given, each extended afterwards by negative feedback (according to the pattern given in Figure 12(a)) and drug inhibition.

The given Petri nets may be read as discrete as well as continuous ones. The essential analysis results of the discrete Petri nets are given directly below the net in the style of the two-column result vector as produced by the Integrated Net Analyser INA [SR99]. By assigning rate functions, the Petri nets turn into continuous ones, describing ODEs. Please note, here we read the place names as real variables, which allows to skip the bracket notation, which is usually used to indicate that the species' concentration is meant and not the species itself. All ODEs are given as produced by Snoopy [Sno], a tool to design and animate hierarchical graphs, especially Petri nets.

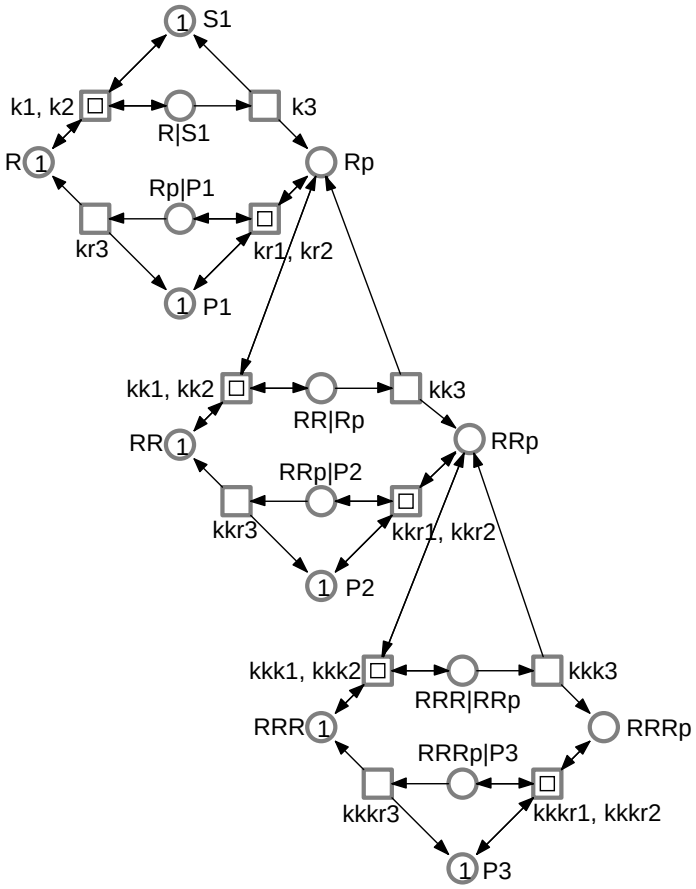


```
ORD HOM NBM PUR CSV SCF CON SC  Ft0 tF0 Fp0 pF0 MG  SM  FC  EFC ES
Y   Y   Y   Y   N   N   Y   Y   N   N   N   N   N   N   N   N   Y
DTP SMC SMD SMA CPI CTI  B  SB  REV DSt BSt DTr DCF  L   LV L&S
Y   Y   Y   Y   Y   Y   Y   Y   Y   N   ?   N   N   Y   Y   Y
----------------------------------------
7 p-invariants
9 t-invariants (6 trivial, 3 non-trivial)
rg: 43 states, 156 arcs, 1 scc
```

Figure 13: Three-stage in vivo cascade (MA1).

ODEs generated by the continuous Petri net given in Figure 13

$$
\begin{aligned}
\frac{d\mathrm{P1}}{d\mathrm{t}} &= \mathrm{kr3} * \mathrm{Rp}|\mathrm{P1} + \mathrm{kr2} * \mathrm{Rp}|\mathrm{P1} - \mathrm{kr1} * \mathrm{Rp} * \mathrm{P1} \\
\frac{d\mathrm{P2}}{d\mathrm{t}} &= \mathrm{kkr3} * \mathrm{RRp}|\mathrm{P2} + \mathrm{kkr2} * \mathrm{RRp}|\mathrm{P2} - \mathrm{kkr1} * \mathrm{RRp} * \mathrm{P2} \\
\frac{d\mathrm{P3}}{d\mathrm{t}} &= \mathrm{kkkr3} * \mathrm{RRRp}|\mathrm{P3} + \mathrm{kkkr2} * \mathrm{RRRp}|\mathrm{P3} - \mathrm{kkkr1} * \mathrm{RRRp} * \mathrm{P3} \\
\frac{d\mathrm{R}}{d\mathrm{t}} &= \mathrm{kr3} * \mathrm{Rp}|\mathrm{P1} + \mathrm{k2} * \mathrm{R}|\mathrm{S1} - \mathrm{k1} * \mathrm{R} * \mathrm{S1} \\
\frac{d\mathrm{RR}}{d\mathrm{t}} &= \mathrm{kkr3} * \mathrm{RRp}|\mathrm{P2} + \mathrm{kk2} * \mathrm{RR}|\mathrm{Rp} - \mathrm{kk1} * \mathrm{RR} * \mathrm{Rp} \\
\frac{d\mathrm{RRR}}{d\mathrm{t}} &= \mathrm{kkkr3} * \mathrm{RRRp}|\mathrm{P3} + \mathrm{kkk2} * \mathrm{RRR}|\mathrm{RRp} - \mathrm{kkk1} * \mathrm{RRR} * \mathrm{RRp} \\
\frac{d\mathrm{RRRp}}{d\mathrm{t}} &= \mathrm{kkk3} * \mathrm{RRR}|\mathrm{RRp} + \mathrm{kkkr2} * \mathrm{RRRp}|\mathrm{P3} - \mathrm{kkkr1} * \mathrm{RRRp} * \mathrm{P3} \\
\frac{d\mathrm{RRRp|P3}}{d\mathrm{t}} &= \mathrm{kkkr1} * \mathrm{RRRp} * \mathrm{P3} - \mathrm{kkkr3} * \mathrm{RRRp}|\mathrm{P3} - \mathrm{kkkr2} * \mathrm{RRRp}|\mathrm{P3} \\
\frac{d\mathrm{RRR|RRp}}{d\mathrm{t}} &= \mathrm{kkk1} * \mathrm{RRR} * \mathrm{RRp} - \mathrm{kkk3} * \mathrm{RRR}|\mathrm{RRp} - \mathrm{kkk2} * \mathrm{RRR}|\mathrm{RRp} \\
\frac{d\mathrm{RRp}}{d\mathrm{t}} &= \mathrm{kk3} * \mathrm{RR}|\mathrm{Rp} + \mathrm{kkk3} * \mathrm{RRR}|\mathrm{RRp} + \mathrm{kkr2} * \mathrm{RRp}|\mathrm{P2} + \\
&\quad \mathrm{kkk2} * \mathrm{RRR}|\mathrm{RRp} - \mathrm{kkr1} * \mathrm{RRp} * \mathrm{P2} - \mathrm{kkk1} * \mathrm{RRR} * \mathrm{RRp} \\
\frac{d\mathrm{RRp|P2}}{d\mathrm{t}} &= \mathrm{kkr1} * \mathrm{RRp} * \mathrm{P2} - \mathrm{kkr3} * \mathrm{RRp}|\mathrm{P2} - \mathrm{kkr2} * \mathrm{RRp}|\mathrm{P2} \\
\frac{d\mathrm{RR|Rp}}{d\mathrm{t}} &= \mathrm{kk1} * \mathrm{RR} * \mathrm{Rp} - \mathrm{kk3} * \mathrm{RR}|\mathrm{Rp} - \mathrm{kk2} * \mathrm{RR}|\mathrm{Rp} \\
\frac{d\mathrm{Rp}}{d\mathrm{t}} &= \mathrm{k3} * \mathrm{R}|\mathrm{S1} + \mathrm{kk3} * \mathrm{RR}|\mathrm{Rp} + \mathrm{kr2} * \mathrm{Rp}|\mathrm{P1} + \mathrm{kk2} * \mathrm{RR}|\mathrm{Rp} - \\
&\quad \mathrm{kr1} * \mathrm{Rp} * \mathrm{P1} - \mathrm{kk1} * \mathrm{RR} * \mathrm{Rp} \\
\frac{d\mathrm{Rp|P1}}{d\mathrm{t}} &= \mathrm{kr1} * \mathrm{Rp} * \mathrm{P1} - \mathrm{kr3} * \mathrm{Rp}|\mathrm{P1} - \mathrm{kr2} * \mathrm{Rp}|\mathrm{P1} \\
\frac{d\mathrm{R|S1}}{d\mathrm{t}} &= \mathrm{k1} * \mathrm{R} * \mathrm{S1} - \mathrm{k3} * \mathrm{R}|\mathrm{S1} - \mathrm{k2} * \mathrm{R}|\mathrm{S1} \\
\frac{d\mathrm{S1}}{d\mathrm{t}} &= \mathrm{k3} * \mathrm{R}|\mathrm{S1} + \mathrm{k2} * \mathrm{R}|\mathrm{S1} - \mathrm{k1} * \mathrm{R} * \mathrm{S1}
\end{aligned}
$$

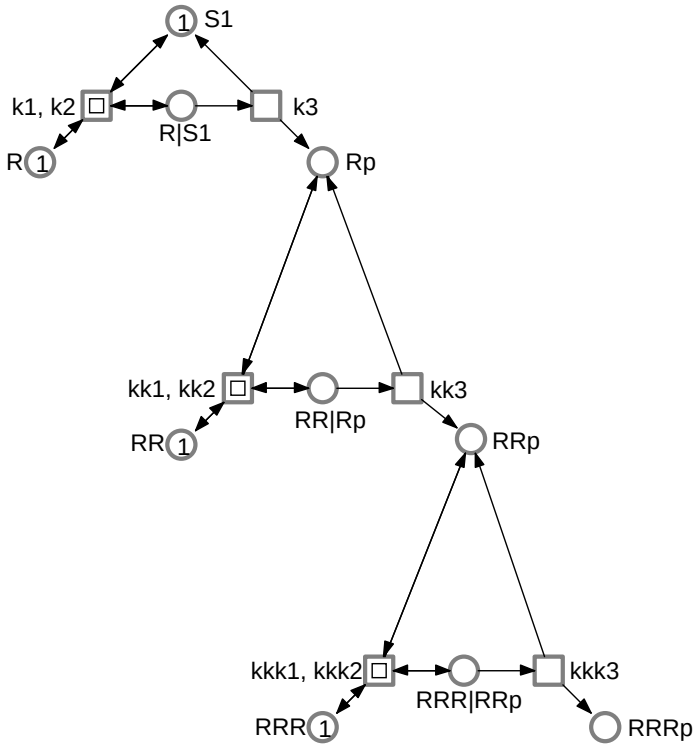


```
ORD HOM NBM PUR CSV SCF CON SC  Ft0 tF0 Fp0 pF0 MG  SM  FC  EFC ES
Y   Y   Y   Y   N   N   Y   N   N   N   N   Y   N   N   Y   Y   Y
DTP SMC SMD SMA CPI CTI  B  SB  REV DSt BSt DTr DCF  L   LV L&S
N   Y   N   N   Y   N   Y   Y   N   Y   ?   N   N   N   N   N
----------------------------------------
4 p-invariants
3 trivial t-invariants
rg: 7 states, 9 arcs, 4 scc's
```

Figure 14: Three-stage in vitro cascade (MA1).

ODEs generated by the continuous Petri net given in Figure 14

$$
\begin{aligned}
\frac{d\mathrm{R}}{d\mathrm{t}} &= \mathrm{k2} * \mathrm{R}|\mathrm{S1} - \mathrm{k1} * \mathrm{R} * \mathrm{S1} \\
\frac{d\mathrm{RR}}{d\mathrm{t}} &= \mathrm{kk2} * \mathrm{RR}|\mathrm{Rp} - \mathrm{kk1} * \mathrm{RR} * \mathrm{Rp} \\
\frac{d\mathrm{RRR}}{d\mathrm{t}} &= \mathrm{kkk2} * \mathrm{RRR}|\mathrm{RRp} - \mathrm{kkk1} * \mathrm{RRR} * \mathrm{RRp} \\
\frac{d\mathrm{RRRp}}{d\mathrm{t}} &= \mathrm{kkk3} * \mathrm{RRR}|\mathrm{RRp} \\
\frac{d\mathrm{RRR}|\mathrm{RRp}}{d\mathrm{t}} &= \mathrm{kkk1} * \mathrm{RRR} * \mathrm{RRp} - \mathrm{kkk3} * \mathrm{RRR}|\mathrm{RRp} - \mathrm{kkk2} * \mathrm{RRR}|\mathrm{RRp} \\
\frac{d\mathrm{RRp}}{d\mathrm{t}} &= \mathrm{kk3} * \mathrm{RR}|\mathrm{Rp} + \mathrm{kkk3} * \mathrm{RRR}|\mathrm{RRp} + \mathrm{kkk2} * \mathrm{RRR}|\mathrm{RRp} - \\
&\quad \mathrm{kkk1} * \mathrm{RRR} * \mathrm{RRp} \\
\frac{d\mathrm{RR}|\mathrm{Rp}}{d\mathrm{t}} &= \mathrm{kk1} * \mathrm{RR} * \mathrm{Rp} - \mathrm{kk3} * \mathrm{RR}|\mathrm{Rp} - \mathrm{kk2} * \mathrm{RR}|\mathrm{Rp} \\
\frac{d\mathrm{Rp}}{d\mathrm{t}} &= \mathrm{k3} * \mathrm{R}|\mathrm{S1} + \mathrm{kk3} * \mathrm{RR}|\mathrm{Rp} + \mathrm{kk2} * \mathrm{RR}|\mathrm{Rp} - \mathrm{kk1} * \mathrm{RR} * \mathrm{Rp} \\
\frac{d\mathrm{R}|\mathrm{S1}}{d\mathrm{t}} &= \mathrm{k1} * \mathrm{R} * \mathrm{S1} - \mathrm{k3} * \mathrm{R}|\mathrm{S1} - \mathrm{k2} * \mathrm{R}|\mathrm{S1} \\
\frac{d\mathrm{S1}}{d\mathrm{t}} &= \mathrm{k3} * \mathrm{R}|\mathrm{S1} + \mathrm{k2} * \mathrm{R}|\mathrm{S1} - \mathrm{k1} * \mathrm{R} * \mathrm{S1}
\end{aligned}
$$

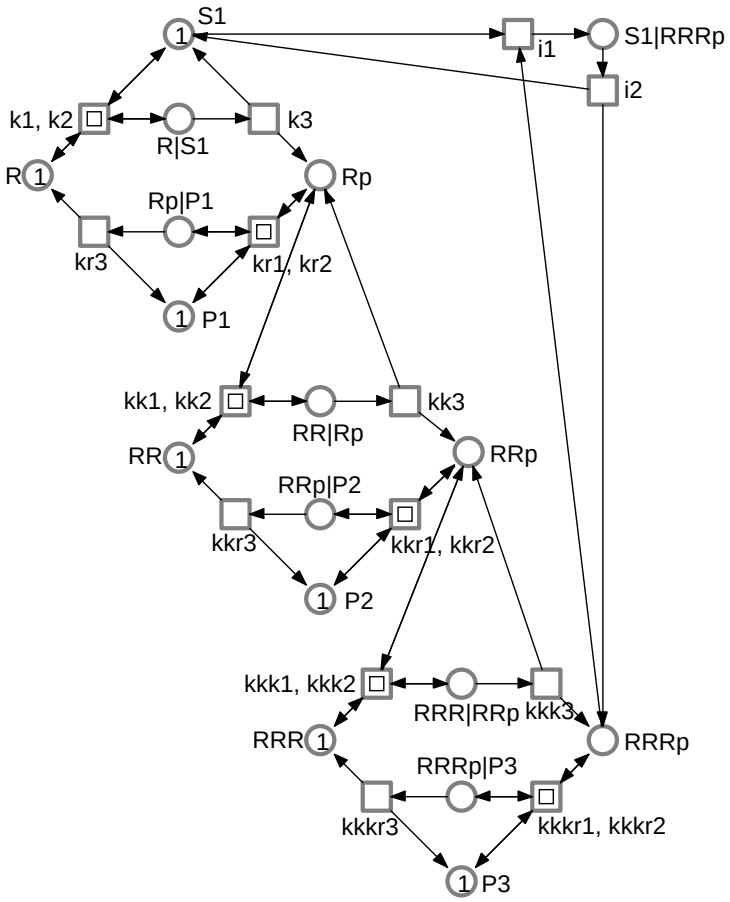


```
ORD HOM NBM PUR CSV SCF CON SC  Ft0 tF0 Fp0 pF0 MG  SM  FC  EFC ES
Y   Y   Y   Y   N   N   Y   Y   N   N   N   N   N   N   N   N   N
DTP SMC SMD SMA CPI CTI  B  SB  REV DSt BSt DTr DCF  L   LV L&S
Y   Y   Y   N   Y   Y   Y   Y   Y   N   ?   N   N   Y   Y   Y
---------------------------------------
7 p-invariants
10 t-invariants (7 trivial, 3 non-trivial)
rg: 53 states, 197 arcs, 1 scc
```

Figure 15: Three-stage in vivo cascade with negative feedback (MA1).

ODEs generated by the continuous Petri net given in Figure 15

$$
\begin{aligned}
\frac{d\mathrm{P1}}{dt} &= \mathrm{kr3} * \mathrm{Rp}|\mathrm{P1} + \mathrm{kr2} * \mathrm{Rp}|\mathrm{P1} - \mathrm{kr1} * \mathrm{Rp} * \mathrm{P1} \\
\frac{d\mathrm{P2}}{dt} &= \mathrm{kkr3} * \mathrm{RRp}|\mathrm{P2} + \mathrm{kkr2} * \mathrm{RRp}|\mathrm{P2} - \mathrm{kkr1} * \mathrm{RRp} * \mathrm{P2} \\
\frac{d\mathrm{P3}}{dt} &= \mathrm{kkkr3} * \mathrm{RRRp}|\mathrm{P3} + \mathrm{kkkr2} * \mathrm{RRRp}|\mathrm{P3} - \mathrm{kkkr1} * \mathrm{RRRp} * \mathrm{P3} \\
\frac{d\mathrm{R}}{dt} &= \mathrm{kr3} * \mathrm{Rp}|\mathrm{P1} + \mathrm{k2} * \mathrm{R}|\mathrm{S1} - \mathrm{k1} * \mathrm{R} * \mathrm{S1} \\
\frac{d\mathrm{RR}}{dt} &= \mathrm{kkr3} * \mathrm{RRp}|\mathrm{P2} + \mathrm{kk2} * \mathrm{RR}|\mathrm{Rp} - \mathrm{kk1} * \mathrm{RR} * \mathrm{Rp} \\
\frac{d\mathrm{RRR}}{dt} &= \mathrm{kkkr3} * \mathrm{RRRp}|\mathrm{P3} + \mathrm{kkk2} * \mathrm{RRR}|\mathrm{RRp} - \mathrm{kkk1} * \mathrm{RRR} * \mathrm{RRp} \\
\frac{d\mathrm{RRRp}}{dt} &= \mathrm{kkk3} * \mathrm{RRR}|\mathrm{RRp} + \mathrm{kkkr2} * \mathrm{RRRp}|\mathrm{P3} + \mathrm{i2} * \mathrm{S1}|\mathrm{RRRp} - \\
&\quad \mathrm{kkkr1} * \mathrm{RRRp} * \mathrm{P3} - \mathrm{i1} * \mathrm{S1} * \mathrm{RRRp} \\
\frac{d\mathrm{RRRp|P3}}{dt} &= \mathrm{kkkr1} * \mathrm{RRRp} * \mathrm{P3} - \mathrm{kkkr3} * \mathrm{RRRp}|\mathrm{P3} - \mathrm{kkkr2} * \mathrm{RRRp}|\mathrm{P3} \\
\frac{d\mathrm{RRR|RRp}}{dt} &= \mathrm{kkk1} * \mathrm{RRR} * \mathrm{RRp} - \mathrm{kkk3} * \mathrm{RRR}|\mathrm{RRp} - \mathrm{kkk2} * \mathrm{RRR}|\mathrm{RRp} \\
\frac{d\mathrm{RRp}}{dt} &= \mathrm{kk3} * \mathrm{RR}|\mathrm{Rp} + \mathrm{kkk3} * \mathrm{RRR}|\mathrm{RRp} + \mathrm{kkr2} * \mathrm{RRp}|\mathrm{P2} + \\
&\quad \mathrm{kkk2} * \mathrm{RRR}|\mathrm{RRp} - \mathrm{kkr1} * \mathrm{RRp} * \mathrm{P2} - \mathrm{kkk1} * \mathrm{RRR} * \mathrm{RRp} \\
\frac{d\mathrm{RRp|P2}}{dt} &= \mathrm{kkr1} * \mathrm{RRp} * \mathrm{P2} - \mathrm{kkr3} * \mathrm{RRp}|\mathrm{P2} - \mathrm{kkr2} * \mathrm{RRp}|\mathrm{P2} \\
\frac{d\mathrm{RR|Rp}}{dt} &= \mathrm{kk1} * \mathrm{RR} * \mathrm{Rp} - \mathrm{kk3} * \mathrm{RR}|\mathrm{Rp} - \mathrm{kk2} * \mathrm{RR}|\mathrm{Rp} \\
\frac{d\mathrm{Rp}}{dt} &= \mathrm{k3} * \mathrm{R}|\mathrm{S1} + \mathrm{kk3} * \mathrm{RR}|\mathrm{Rp} + \mathrm{kr2} * \mathrm{Rp}|\mathrm{P1} + \mathrm{kk2} * \mathrm{RR}|\mathrm{Rp} - \\
&\quad \mathrm{kr1} * \mathrm{Rp} * \mathrm{P1} - \mathrm{kk1} * \mathrm{RR} * \mathrm{Rp} \\
\frac{d\mathrm{Rp|P1}}{dt} &= \mathrm{kr1} * \mathrm{Rp} * \mathrm{P1} - \mathrm{kr3} * \mathrm{Rp}|\mathrm{P1} - \mathrm{kr2} * \mathrm{Rp}|\mathrm{P1} \\
\frac{d\mathrm{R|S1}}{dt} &= \mathrm{k1} * \mathrm{R} * \mathrm{S1} - \mathrm{k3} * \mathrm{R}|\mathrm{S1} - \mathrm{k2} * \mathrm{R}|\mathrm{S1} \\
\frac{d\mathrm{S1}}{dt} &= \mathrm{k3} * \mathrm{R}|\mathrm{S1} + \mathrm{k2} * \mathrm{R}|\mathrm{S1} + \mathrm{i2} * \mathrm{S1}|\mathrm{RRRp} - \mathrm{k1} * \mathrm{R} * \mathrm{S1} - \\
&\quad \mathrm{i1} * \mathrm{S1} * \mathrm{RRRp} \\
\frac{d\mathrm{S1|RRRp}}{dt} &= \mathrm{i1} * \mathrm{S1} * \mathrm{RRRp} - \mathrm{i2} * \mathrm{S1}|\mathrm{RRRp}
\end{aligned}
$$

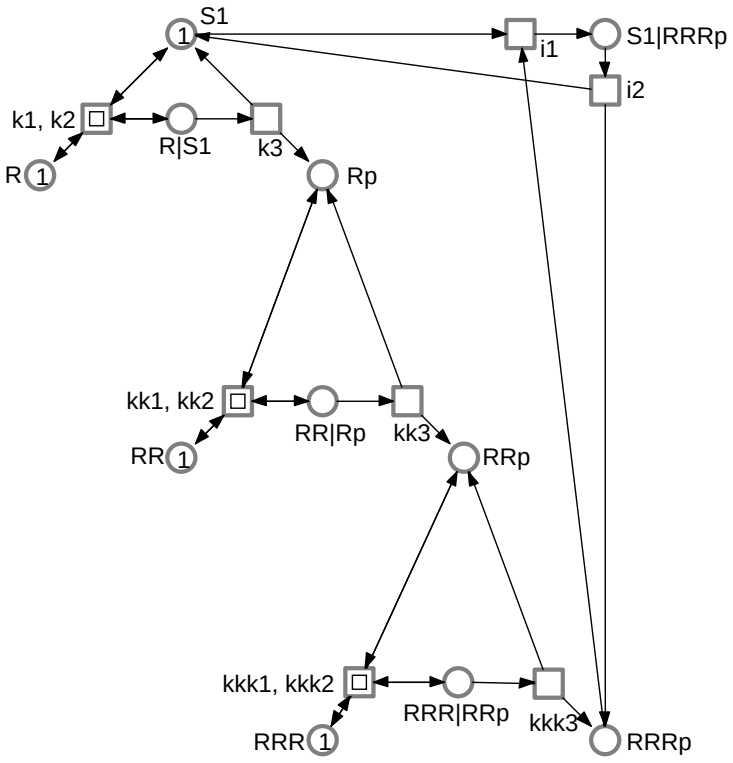


```
ORD HOM NBM PUR CSV SCF CON SC  Ft0 tF0 Fp0 pF0 MG  SM  FC  EFC ES
Y   Y   Y   Y   N   N   Y   Y   N   N   N   N   N   N   N   N   Y
DTP SMC SMD SMA CPI CTI  B  SB  REV DSt BSt DTr DCF  L   LV L&S
N   ?   N   N   Y   N   Y   Y   N   N   ?   N   N   N   N   N
-----------------------------------------
4 p-invariants
4 trivial t-invariants
rg: 8 states, 11 arcs, 4 scc's
```

Figure 16: Three-stage in vitro cascade with negative feedback (MA1).

ODEs generated by the continuous Petri net given in Figure 16

$$
\begin{aligned}
\frac{d\mathrm{R}}{d\mathrm{t}} &= \mathrm{k2} * \mathrm{R}|\mathrm{S1} - \mathrm{k1} * \mathrm{R} * \mathrm{S1} \\
\frac{d\mathrm{RR}}{d\mathrm{t}} &= \mathrm{kk2} * \mathrm{RR}|\mathrm{Rp} - \mathrm{kk1} * \mathrm{RR} * \mathrm{Rp} \\
\frac{d\mathrm{RRR}}{d\mathrm{t}} &= \mathrm{kkk2} * \mathrm{RRR}|\mathrm{RRp} - \mathrm{kkk1} * \mathrm{RRR} * \mathrm{RRp} \\
\frac{d\mathrm{RRRp}}{d\mathrm{t}} &= \mathrm{kkk3} * \mathrm{RRR}|\mathrm{RRp} + \mathrm{i2} * \mathrm{S1}|\mathrm{RRRp} - \mathrm{i1} * \mathrm{S1} * \mathrm{RRRp} \\
\frac{d\mathrm{RRR|RRp}}{d\mathrm{t}} &= \mathrm{kkk1} * \mathrm{RRR} * \mathrm{RRp} - \mathrm{kkk3} * \mathrm{RRR}|\mathrm{RRp} - \mathrm{kkk2} * \mathrm{RRR}|\mathrm{RRp} \\
\frac{d\mathrm{RRp}}{d\mathrm{t}} &= \mathrm{kk3} * \mathrm{RR}|\mathrm{Rp} + \mathrm{kkk3} * \mathrm{RRR}|\mathrm{RRp} + \mathrm{kkk2} * \mathrm{RRR}|\mathrm{RRp} - \\
&\quad \mathrm{kkk1} * \mathrm{RRR} * \mathrm{RRp} \\
\frac{d\mathrm{RR}|\mathrm{Rp}}{d\mathrm{t}} &= \mathrm{kk1} * \mathrm{RR} * \mathrm{Rp} - \mathrm{kk3} * \mathrm{RR}|\mathrm{Rp} - \mathrm{kk2} * \mathrm{RR}|\mathrm{Rp} \\
\frac{d\mathrm{Rp}}{d\mathrm{t}} &= \mathrm{k3} * \mathrm{R}|\mathrm{S1} + \mathrm{kk3} * \mathrm{RR}|\mathrm{Rp} + \mathrm{kk2} * \mathrm{RR}|\mathrm{Rp} - \mathrm{kk1} * \mathrm{RR} * \mathrm{Rp} \\
\frac{d\mathrm{R}|\mathrm{S1}}{d\mathrm{t}} &= \mathrm{k1} * \mathrm{R} * \mathrm{S1} - \mathrm{k3} * \mathrm{R}|\mathrm{S1} - \mathrm{k2} * \mathrm{R}|\mathrm{S1} \\
\frac{d\mathrm{S1}}{d\mathrm{t}} &= \mathrm{k3} * \mathrm{R}|\mathrm{S1} + \mathrm{k2} * \mathrm{R}|\mathrm{S1} + \mathrm{i2} * \mathrm{S1}|\mathrm{RRRp} - \mathrm{k1} * \mathrm{R} * \mathrm{S1} - \\
&\quad \mathrm{i1} * \mathrm{S1} * \mathrm{RRRp} \\
\frac{d\mathrm{S1}|\mathrm{RRRp}}{d\mathrm{t}} &= \mathrm{i1} * \mathrm{S1} * \mathrm{RRRp} - \mathrm{i2} * \mathrm{S1}|\mathrm{RRRp}
\end{aligned}
$$

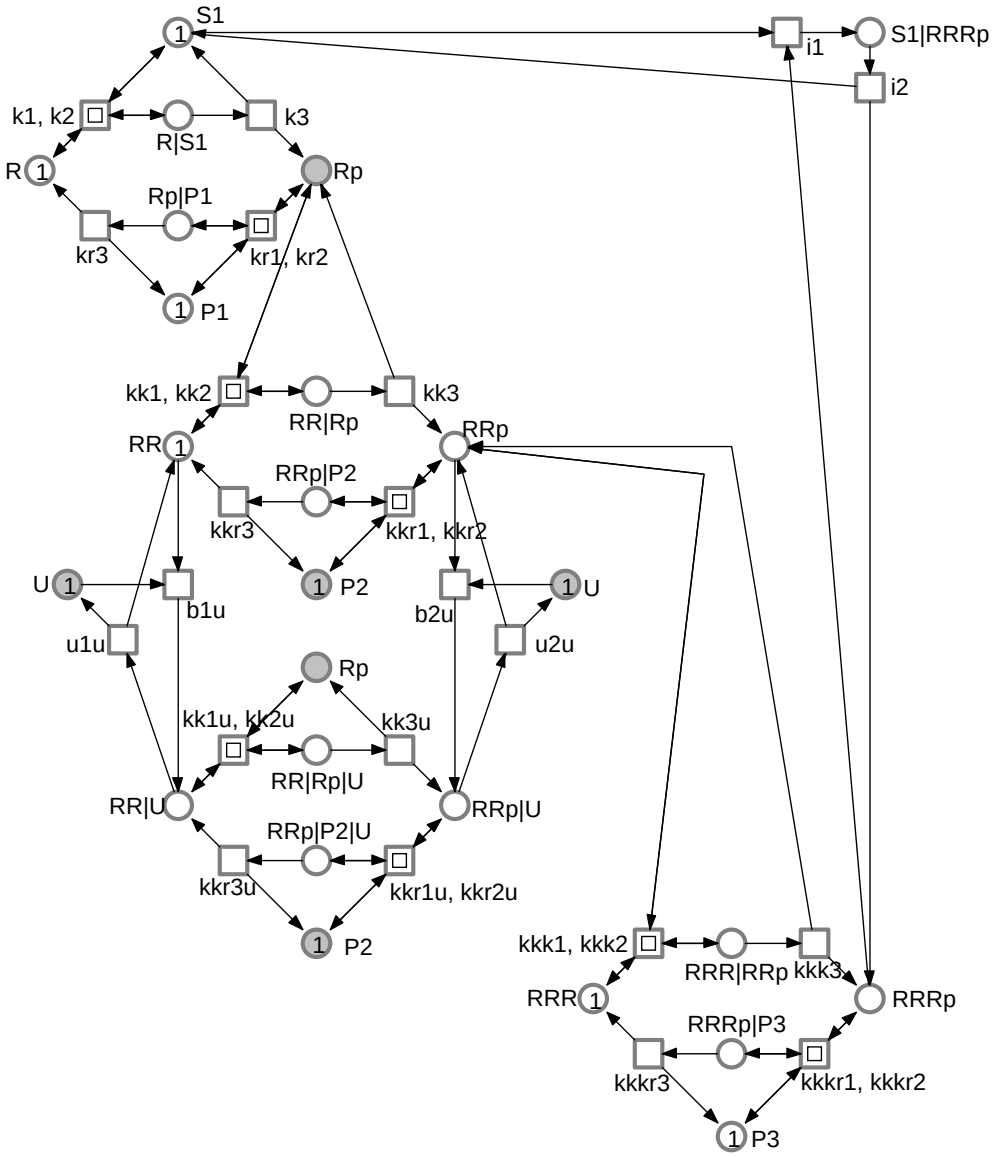


```
ORD HOM NBM PUR CSV SCF CON SC  Ft0 tF0 Fp0 pF0 MG  SM  FC  EFC ES
Y   Y   Y   Y   N   N   Y   Y   N   N   N   N   N   N   N   N   N
DTP SMC SMD SMA CPI CTI  B  SB  REV DSt BSt DTr DCF  L   LV L&S
Y   Y   Y   N   Y   Y   Y   Y   Y   N   ?   N   N   Y   Y   Y
---------------------------------------
8 p-invariants
17 t-invariants (11 trivial, 6 non-trivial)
rg: 102 states, 436 arcs, 1 scc
```

Figure 17: Three-stage in vivo cascade with negative feedback and drug inhibition (MA1). The nodes given in gray indicate logical nodes (also called fusion nodes). Logical nodes with identical names are from a structural point of view identical; they are used to increase readability in larger net structures by connecting logically remote net parts.

ODEs generated by the continuous Petri net given in Figure 17

$$
\begin{aligned}
\frac{d\mathrm{P1}}{dt} &= \mathrm{kr3} * \mathrm{Rp}|\mathrm{P1} + \mathrm{kr2} * \mathrm{Rp}|\mathrm{P1} - \mathrm{kr1} * \mathrm{Rp} * \mathrm{P1} \\
\frac{d\mathrm{P2}}{dt} &= \mathrm{kkr3} * \mathrm{RRp}|\mathrm{P2} + \mathrm{kkr2} * \mathrm{RRp}|\mathrm{P2} + \mathrm{kkr3u} * \mathrm{RRp}|\mathrm{P2}|\mathrm{U} + \\
&\quad \mathrm{kkr2u} * \mathrm{RRp}|\mathrm{P2}|\mathrm{U} - \mathrm{kkr1} * \mathrm{RRp} * \mathrm{P2} - \mathrm{kkr1u} * \mathrm{RRp}|\mathrm{U} * \mathrm{P2} \\
\frac{d\mathrm{P3}}{dt} &= \mathrm{kkkr3} * \mathrm{RRRp}|\mathrm{P3} + \mathrm{kkkr2} * \mathrm{RRRp}|\mathrm{P3} - \mathrm{kkkr1} * \mathrm{RRRp} * \mathrm{P3} \\
\frac{d\mathrm{R}}{dt} &= \mathrm{kr3} * \mathrm{Rp}|\mathrm{P1} + \mathrm{k2} * \mathrm{R}|\mathrm{S1} - \mathrm{k1} * \mathrm{R} * \mathrm{S1} \\
\frac{d\mathrm{RR}}{dt} &= \mathrm{kkr3} * \mathrm{RRp}|\mathrm{P2} + \mathrm{kk2} * \mathrm{RR}|\mathrm{Rp} + \mathrm{u1u} * \mathrm{RR}|\mathrm{U} - \mathrm{kk1} * \mathrm{RR} * \mathrm{Rp} - \\
&\quad \mathrm{b1u} * \mathrm{RR} * \mathrm{U} \\
\frac{d\mathrm{RRR}}{dt} &= \mathrm{kkkr3} * \mathrm{RRRp}|\mathrm{P3} + \mathrm{kkk2} * \mathrm{RRR}|\mathrm{RRp} - \mathrm{kkk1} * \mathrm{RRR} * \mathrm{RRp} \\
\frac{d\mathrm{RRRp}}{dt} &= \mathrm{kkk3} * \mathrm{RRR}|\mathrm{RRp} + \mathrm{kkkr2} * \mathrm{RRRp}|\mathrm{P3} + \mathrm{i2} * \mathrm{S1}|\mathrm{RRRp} - \\
&\quad \mathrm{kkkr1} * \mathrm{RRRp} * \mathrm{P3} - \mathrm{i1} * \mathrm{S1} * \mathrm{RRRp} \\
\frac{d\mathrm{RRRp}|\mathrm{P3}}{dt} &= \mathrm{kkkr1} * \mathrm{RRRp} * \mathrm{P3} - \mathrm{kkkr3} * \mathrm{RRRp}|\mathrm{P3} - \mathrm{kkkr2} * \mathrm{RRRp}|\mathrm{P3} \\
\frac{d\mathrm{RRR}|\mathrm{RRp}}{dt} &= \mathrm{kkk1} * \mathrm{RRR} * \mathrm{RRp} - \mathrm{kkk3} * \mathrm{RRR}|\mathrm{RRp} - \mathrm{kkk2} * \mathrm{RRR}|\mathrm{RRp} \\
\frac{d\mathrm{RRp}}{dt} &= \mathrm{kk3} * \mathrm{RR}|\mathrm{Rp} + \mathrm{kkk3} * \mathrm{RRR}|\mathrm{RRp} + \mathrm{kkr2} * \mathrm{RRp}|\mathrm{P2} + \mathrm{kkk2} * \mathrm{RRR}|\mathrm{RRp} + \\
&\quad \mathrm{u2u} * \mathrm{RRp}|\mathrm{U} - \mathrm{kkr1} * \mathrm{RRp} * \mathrm{P2} - \mathrm{kkk1} * \mathrm{RRR} * \mathrm{RRp} - \mathrm{b2u} * \mathrm{RRp} * \mathrm{U} \\
\frac{d\mathrm{RRp}|\mathrm{P2}}{dt} &= \mathrm{kkr1} * \mathrm{RRp} * \mathrm{P2} - \mathrm{kkr3} * \mathrm{RRp}|\mathrm{P2} - \mathrm{kkr2} * \mathrm{RRp}|\mathrm{P2} \\
\frac{d\mathrm{RRp}|\mathrm{P2}|\mathrm{U}}{dt} &= \mathrm{kkr1u} * \mathrm{RRp}|\mathrm{U} * \mathrm{P2} - \mathrm{kkr3u} * \mathrm{RRp}|\mathrm{P2}|\mathrm{U} - \mathrm{kkr2u} * \mathrm{RRp}|\mathrm{P2}|\mathrm{U} \\
\frac{d\mathrm{RRp}|\mathrm{U}}{dt} &= \mathrm{kk3u} * \mathrm{RR}|\mathrm{Rp}|\mathrm{U} + \mathrm{b2u} * \mathrm{RRp} * \mathrm{U} + \mathrm{kkr2u} * \mathrm{RRp}|\mathrm{P2}|\mathrm{U} - \mathrm{u2u} * \mathrm{RRp}|\mathrm{U} - \\
&\quad \mathrm{kkr1u} * \mathrm{RRp}|\mathrm{U} * \mathrm{P2} \\
\frac{d\mathrm{RR}|\mathrm{Rp}}{dt} &= \mathrm{kk1} * \mathrm{RR} * \mathrm{Rp} - \mathrm{kk3} * \mathrm{RR}|\mathrm{Rp} - \mathrm{kk2} * \mathrm{RR}|\mathrm{Rp} \\
\frac{d\mathrm{RR}|\mathrm{Rp}|\mathrm{U}}{dt} &= \mathrm{kk1u} * \mathrm{RR}|\mathrm{U} * \mathrm{Rp} - \mathrm{kk3u} * \mathrm{RR}|\mathrm{Rp}|\mathrm{U} - \mathrm{kk2u} * \mathrm{RR}|\mathrm{Rp}|\mathrm{U} \\
\frac{d\mathrm{RR}|\mathrm{U}}{dt} &= \mathrm{b1u} * \mathrm{RR} * \mathrm{U} + \mathrm{kkr3u} * \mathrm{RRp}|\mathrm{P2}|\mathrm{U} + \mathrm{kk2u} * \mathrm{RR}|\mathrm{Rp}|\mathrm{U} - \mathrm{u1u} * \mathrm{RR}|\mathrm{U} - \\
&\quad \mathrm{kk1u} * \mathrm{RR}|\mathrm{U} * \mathrm{Rp} \\
\frac{d\mathrm{Rp}}{dt} &= \mathrm{k3} * \mathrm{R}|\mathrm{S1} + \mathrm{kk3} * \mathrm{RR}|\mathrm{Rp} + \mathrm{kr2} * \mathrm{Rp}|\mathrm{P1} + \mathrm{kk2} * \mathrm{RR}|\mathrm{Rp} + \\
&\quad \mathrm{kk2u} * \mathrm{RR}|\mathrm{Rp}|\mathrm{U} + \mathrm{kk3u} * \mathrm{RR}|\mathrm{Rp}|\mathrm{U} - \mathrm{kr1} * \mathrm{Rp} * \mathrm{P1} - \mathrm{kk1} * \mathrm{RR} * \mathrm{Rp} - \\
&\quad \mathrm{kk1u} * \mathrm{RR}|\mathrm{U} * \mathrm{Rp} \\
\frac{d\mathrm{Rp}|\mathrm{P1}}{dt} &= \mathrm{kr1} * \mathrm{Rp} * \mathrm{P1} - \mathrm{kr3} * \mathrm{Rp}|\mathrm{P1} - \mathrm{kr2} * \mathrm{Rp}|\mathrm{P1} \\
\frac{d\mathrm{R}|\mathrm{S1}}{dt} &= \mathrm{k1} * \mathrm{R} * \mathrm{S1} - \mathrm{k3} * \mathrm{R}|\mathrm{S1} - \mathrm{k2} * \mathrm{R}|\mathrm{S1} \\
\frac{d\mathrm{S1}}{dt} &= \mathrm{k3} * \mathrm{R}|\mathrm{S1} + \mathrm{k2} * \mathrm{R}|\mathrm{S1} + \mathrm{i2} * \mathrm{S1}|\mathrm{RRRp} - \mathrm{k1} * \mathrm{R} * \mathrm{S1} - \mathrm{i1} * \mathrm{S1} * \mathrm{RRRp} \\
\frac{d\mathrm{S1}|\mathrm{RRRp}}{dt} &= \mathrm{i1} * \mathrm{S1} * \mathrm{RRRp} - \mathrm{i2} * \mathrm{S1}|\mathrm{RRRp} \\
\frac{d\mathrm{U}}{dt} &= \mathrm{u1u} * \mathrm{RR}|\mathrm{U} + \mathrm{u2u} * \mathrm{RRp}|\mathrm{U} - \mathrm{b1u} * \mathrm{RR} * \mathrm{U} - \mathrm{b2u} * \mathrm{RRp} * \mathrm{U}
\end{aligned}
$$

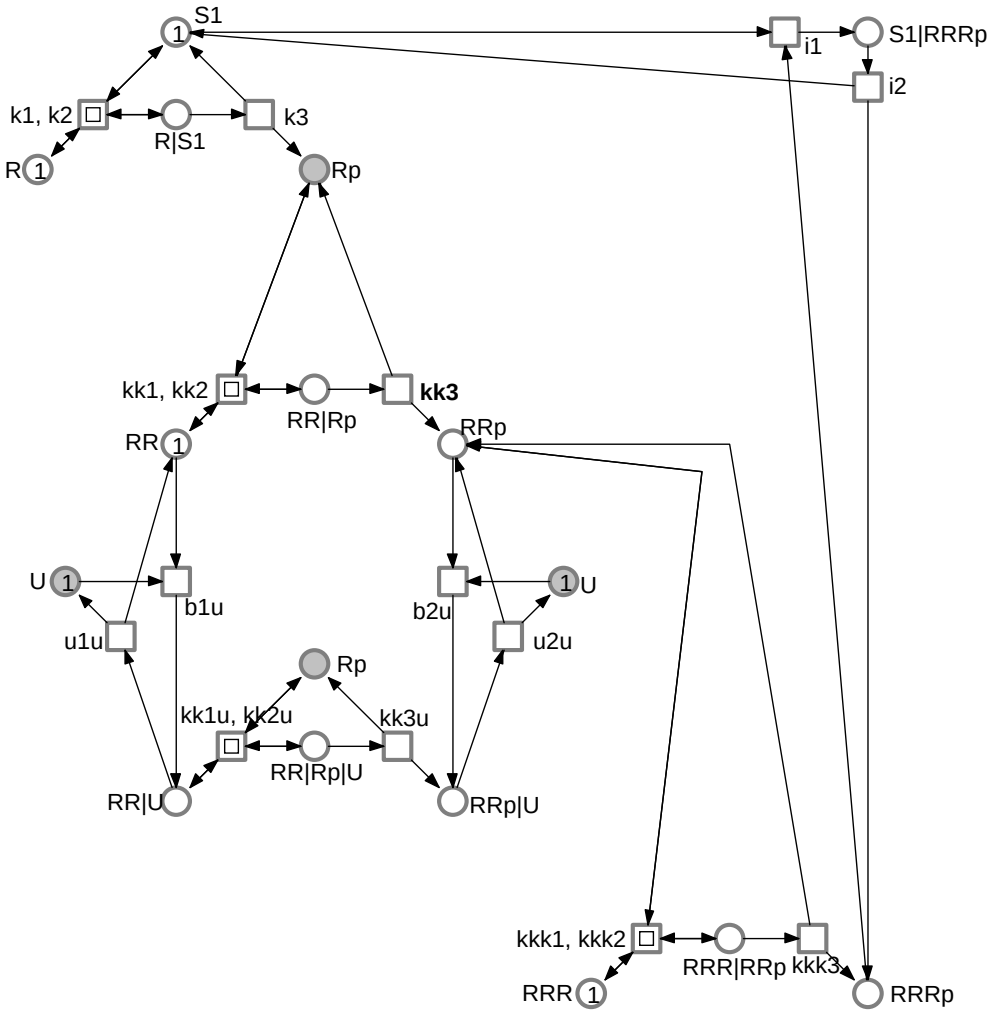


```
ORD HOM NBM PUR CSV SCF CON SC  Ft0 tF0 Fp0 pF0 MG  SM  FC  EFC ES
Y   Y   Y   Y   N   N   Y   Y   N   N   N   N   N   N   N   N   N
DTP SMC SMD SMA CPI CTI  B  SB  REV DSt BSt DTr DCF  L   LV L&S
N   Y   N   N   Y   N   Y   Y   N   N   ?   N   N   N   N   N
-----------------------------------------
5 p-invariants
7 trivial t-invariants
rg: 15 states, 31 arcs, 4 scc's
```

Figure 18: Three-stage in vitro cascade with negative feedback and drug inhibition (MA1).

ODEs generated by the continuous Petri net given in Figure 18

$$
\begin{aligned}
\frac{d\mathrm{R}}{d\mathrm{t}} &= \mathrm{k2} * \mathrm{R}|\mathrm{S1} - \mathrm{k1} * \mathrm{R} * \mathrm{S1} \\
\frac{d\mathrm{RR}}{d\mathrm{t}} &= \mathrm{kk2} * \mathrm{RR}|\mathrm{Rp} + \mathrm{u1u} * \mathrm{RR}|\mathrm{U} - \mathrm{kk1} * \mathrm{RR} * \mathrm{Rp} - \mathrm{b1u} * \mathrm{RR} * \mathrm{U} \\
\frac{d\mathrm{RRR}}{d\mathrm{t}} &= \mathrm{kkk2} * \mathrm{RRR}|\mathrm{RRp} - \mathrm{kkk1} * \mathrm{RRR} * \mathrm{RRp} \\
\frac{d\mathrm{RRRp}}{d\mathrm{t}} &= \mathrm{kkk3} * \mathrm{RRR}|\mathrm{RRp} + \mathrm{i2} * \mathrm{S1}|\mathrm{RRRp} - \mathrm{i1} * \mathrm{S1} * \mathrm{RRRp} \\
\frac{d\mathrm{RRR}|\mathrm{RRp}}{d\mathrm{t}} &= \mathrm{kkk1} * \mathrm{RRR} * \mathrm{RRp} - \mathrm{kkk3} * \mathrm{RRR}|\mathrm{RRp} - \mathrm{kkk2} * \mathrm{RRR}|\mathrm{RRp} \\
\frac{d\mathrm{RRp}}{d\mathrm{t}} &= \mathrm{kk3} * \mathrm{RR}|\mathrm{Rp} + \mathrm{kkk3} * \mathrm{RRR}|\mathrm{RRp} + \mathrm{kkk2} * \mathrm{RRR}|\mathrm{RRp} + \\
&\quad \mathrm{u2u} * \mathrm{RRp}|\mathrm{U} - \mathrm{kkk1} * \mathrm{RRR} * \mathrm{RRp} - \mathrm{b2u} * \mathrm{RRp} * \mathrm{U} \\
\frac{d\mathrm{RRp}|\mathrm{U}}{d\mathrm{t}} &= \mathrm{kk3u} * \mathrm{RR}|\mathrm{Rp}|\mathrm{U} + \mathrm{b2u} * \mathrm{RRp} * \mathrm{U} - \mathrm{u2u} * \mathrm{RRp}|\mathrm{U} \\
\frac{d\mathrm{RR}|\mathrm{Rp}}{d\mathrm{t}} &= \mathrm{kk1} * \mathrm{RR} * \mathrm{Rp} - \mathrm{kk3} * \mathrm{RR}|\mathrm{Rp} - \mathrm{kk2} * \mathrm{RR}|\mathrm{Rp} \\
\frac{d\mathrm{RR}|\mathrm{Rp}|\mathrm{U}}{d\mathrm{t}} &= \mathrm{kk1u} * \mathrm{RR}|\mathrm{U} * \mathrm{Rp} - \mathrm{kk3u} * \mathrm{RR}|\mathrm{Rp}|\mathrm{U} - \mathrm{kk2u} * \mathrm{RR}|\mathrm{Rp}|\mathrm{U} \\
\frac{d\mathrm{RR}|\mathrm{U}}{d\mathrm{t}} &= \mathrm{b1u} * \mathrm{RR} * \mathrm{U} + \mathrm{kk2u} * \mathrm{RR}|\mathrm{Rp}|\mathrm{U} - \mathrm{u1u} * \mathrm{RR}|\mathrm{U} - \\
&\quad \mathrm{kk1u} * \mathrm{RR}|\mathrm{U} * \mathrm{Rp} \\
\frac{d\mathrm{Rp}}{d\mathrm{t}} &= \mathrm{k3} * \mathrm{R}|\mathrm{S1} + \mathrm{kk3} * \mathrm{RR}|\mathrm{Rp} + \mathrm{kk2} * \mathrm{RR}|\mathrm{Rp} + \mathrm{kk2u} * \mathrm{RR}|\mathrm{Rp}|\mathrm{U} + \\
&\quad \mathrm{kk3u} * \mathrm{RR}|\mathrm{Rp}|\mathrm{U} - \mathrm{kk1} * \mathrm{RR} * \mathrm{Rp} - \mathrm{kk1u} * \mathrm{RR}|\mathrm{U} * \mathrm{Rp} \\
\frac{d\mathrm{R}|\mathrm{S1}}{d\mathrm{t}} &= \mathrm{k1} * \mathrm{R} * \mathrm{S1} - \mathrm{k3} * \mathrm{R}|\mathrm{S1} - \mathrm{k2} * \mathrm{R}|\mathrm{S1} \\
\frac{d\mathrm{S1}}{d\mathrm{t}} &= \mathrm{k3} * \mathrm{R}|\mathrm{S1} + \mathrm{k2} * \mathrm{R}|\mathrm{S1} + \mathrm{i2} * \mathrm{S1}|\mathrm{RRRp} - \mathrm{k1} * \mathrm{R} * \mathrm{S1} - \\
&\quad \mathrm{i1} * \mathrm{S1} * \mathrm{RRRp} \\
\frac{d\mathrm{S1}|\mathrm{RRRp}}{d\mathrm{t}} &= \mathrm{i1} * \mathrm{S1} * \mathrm{RRRp} - \mathrm{i2} * \mathrm{S1}|\mathrm{RRRp} \\
\frac{d\mathrm{U}}{d\mathrm{t}} &= \mathrm{u1u} * \mathrm{RR}|\mathrm{U} + \mathrm{u2u} * \mathrm{RRp}|\mathrm{U} - \mathrm{b1u} * \mathrm{RR} * \mathrm{U} - \mathrm{b2u} * \mathrm{RRp} * \mathrm{U}
\end{aligned}
$$